Unusual winter Saharan dust intrusions at Northwest Spain: Air quality, radiative and health impacts

F. Oduber, A.I. Calvo, C. Blanco-Alegre, A. Castro, T. Nunes, C. Alves, M. Sorribas, D. Fernández-González, A.M. Vega-Maray, R.M. Valencia-Barrera, F. Lucarelli, S. Nava, G. Calzolai, E. Alonso-Blanco, B. Fraile, P. Fialho, E. Coz, A.S.H. Prevot, V. Pont, R. Fraile

PII: S0048-9697(19)30804-6
DOI: https://doi.org/10.1016/j.scitotenv.2019.02.305
Reference: STOTEN 31051

To appear in: *Science of the Total Environment*

Received date: 23 December 2018
Revised date: 16 February 2019
Accepted date: 19 February 2019

Please cite this article as: F. Oduber, A.I. Calvo, C. Blanco-Alegre, et al., Unusual winter Saharan dust intrusions at Northwest Spain: Air quality, radiative and health impacts, Science of the Total Environment, https://doi.org/10.1016/j.scitotenv.2019.02.305

Unusual winter Saharan dust intrusions at Northwest Spain: air quality, radiative and health impacts

F. Oduber[1], A. I. Calvo[1], C. Blanco-Alegre[1], A. Castro[1], T. Nunes[2], C. Alves[2], M. Sorribas[3], D. Fernández-González[4,5], A.M. Vega-Maray[4], R.M. Valencia-Barrera[4], F. Lucarelli[6], S. Nava[6], G. Calzolai[6], E. Alonso-Blanco[7], B. Fraile[8], P. Fialho[9], E. Coz[7], A.S.H. Prevot[10], V. Pont[11], R. Fraile[1]

[1]Department of Physics, IMARENAB University of León, León, Spain.

[2]Centre for Environmental and Marine Studies, Department of Environment, University of Aveiro, Aveiro, Portugal.

[3]El Arenosillo- Atmospheric Sounding Station, Atmospheric Research and Instrumentation Branch, INTA, Mazagón-Huelva, Spain.

[4]Biodiversity and Environmental Management, University of León, Spain

[5]Institute of Atmospheric Sciences and Climate-CNR, Bologna, Italy

[6]Department of Physics and Astronomy, University of Florence and I.N.F.N., Florence, Italy

[7]Centre for Energy, Environment and Technology Research (CIEMAT), Department of the Environment, Madrid, Spain

[8]Department of Biomedicine and Biotechnology, University of Alcalá, Alcalá de Henares, Spain

[9]Research Institute for Volcanology and Risk Assessment– IVAR, Ponta Delgada, Portugal

[10]Laboratory of Atmospheric Chemistry, Paul Scherrer Institute, Villigen, Switzerland

[11] Laboratory of Aerology, National Center for Scientific Research (CNRS), University of Toulouse, Toulouse, France

Corresponding author:

Roberto Fraile

Tel: +34 987 291 543

e-mail: roberto.fraile@unileon.es

Abstract

Saharan air masses can transport high amounts of mineral dust particles and biological material to the Iberian Peninsula. During winter, this kind of events is not very frequent and usually does not reach the northwest of the Peninsula. However, between 21 and 22 February 2016 and between 22 and 23 February 2017, two exceptional events were registered in León (Spain), which severely affected air quality. An integrative approach including: i) typical synoptic conditions; ii) aerosol chemical composition; iii) particle size distributions; iv) pollen concentration; v) aerosol optical depth (AOD); vi) radiative forcing and vii) estimation of the impact of aerosols in the respiratory tract, was carried out. In the global characterization of these events, the exceedance of the PM_{10} daily limit value, an increase in the coarse mode and a rise in the iron concentration were observed. On the 2016 event, an AOD and extinction-related Ångström exponent clearly characteristic of desert aerosol (1.1 and 0.05, respectively) was registered. Furthermore, pollen grains not typical of flowering plants in this period were identified. The chemical analysis of the aerosol from the 2017 event allowed us to confirm the presence of the main elements associated with mineral sources (aluminum, calcium, and silica concentrations). An increase in the SO_4^{2-}, NO_3^- and Cl^- concentrations during the Saharan dust intrusion was also noted. However, in this event, there was no presence of atypical pollen types. The estimated dust radiative forcing traduced a cooling effect for surface and atmosphere during both events, corroborated by trends of radiative flux measurements. The estimated impact in the respiratory tract regions of the high levels of particulate matter during both Saharan dust intrusions showed high levels for the respirable fraction.

Keywords: aerosol optical properties, bioaerosol, particle size distribution, radiative forcing, respirable fraction, winter dust intrusion.

1. Introduction

The Intergovernmental Panel on Climate Change (IPCC) fourth assessment report suggests that one of the major natural sources of particles is mineral dust, which comes from dry continental areas. Moreover, the acceleration of the desertification process in arid regions, due to climate change, can result in a rise of dust outbreaks (IPCC, 2014).

Desert dust outbreaks represent a high risk to human health and can cause respiratory and cardiovascular disorders (Goudie, 2014; Jiménez et al., 2010; Stafoggia et al., 2015; Tobías et al., 2011). The effect of particles from mineral dust is related to their chemical composition and size (Díaz et al., 2017; Griffin, 2007; López-Villarrubia et al., 2012; Perez et al., 2008). Depending on their size, they can reach different parts of the respiratory system (ISO, 1995) and, consequently, cause different effects on the human health (Fubini and Otero, 1999). Besides, desert dust is mainly composed of calcite ($CaCO_3$), dolomite ($CaMgCO_3$), quartz (SiO_2) and clay minerals (Calvo et al., 2013; Caquineau et al., 1998; Coz et al., 2009; Glaccum and Prospero, 1980; Guerzoni et al., 1997; Schütz and Sebert, 1987), which are related to asthma and silicosis (Fubini and Otero, 1999).

The high exposure risk during outbreaks is also associated with the biological material mixed with the dust (Garrison et al., 2006; Griffin, 2007; Griffin et al., 2001; Polymenakou et al., 2007). Dust storms can transport bacteria, pollen spores, fungi and viruses, which are capable of surviving long-range transport (Tomadin et al., 1989). The presence of this biological material in small size particles have a potential implication on human health, and may have direct incidence in diseases as meningococcal meningitis and coccidioidomycosis (Goudie, 2014; Polymenakou et al., 2007).

African dust is one of the natural causes of the exceedances in the PM_{10} daily limit value (DLV, 50 μg m^3 set by the Directive 2008/50/EC) in the Iberian Peninsula (Escudero et al., 2007; Nicolás et al., 2008; Querol et al., 2004a; Salvador et al., 2013). Studies carried out by Alastuey et al. (2016) between 2012 and 2013 in different European cities show that, during dust outbreaks, southern and eastern countries have the most elevated concentrations of PM_{10} mineral dust (20- 40% of PM_{10}), due to the proximity to the dust sources. The magnitude of these events depends on several factors (surface wind speed, vegetation cover, soil texture and moisture).

Spain is frequently affected by Saharan dust outbreaks, due to its proximity to large emitting areas (Sahara and Sahel desert) and the meteorological and dynamical characteristics of the atmosphere (Alastuey et al., 2016; Escudero et al., 2007; Querol et al., 2014; Rodríguez et al., 2001). Southern cities are more affected than northern ones (Viana et al., 2014). Stafoggia et al. (2015) and Nicolás et al. (2008) reported an increase in the PM_{10} mass concentrations during dust outbreaks episodes in southern and southeastern Spain, with a contribution of mineral dust between 5 to 40% of the total PM_{10} mass. Moreover, Querol et al. (2004a) showed that the African dust outbreaks are less frequent in the north of Spain than in the south, with an average of 6 and 17 episodes per year, respectively. Most of these events occur between spring and summer, when the dust transportation is governed by the anticyclonic activities over the east or southeast of Iberian Peninsula (Lyamani et al., 2015; Rodríguez et al., 2001; Salvador et al., 2013), with a mean duration of 5-19 days in the south and less than 4 days in the north of Spain (Querol et al., 2004a). In winter, Saharan dust intrusions are scarce and usually do not reach the northwest of the peninsula. Furthermore, they are

governed by the cyclonic activities over the west or south of Portugal (Díaz et al., 2017; Rodríguez et al., 2001). These episodes are characterized by a short duration (between 2-5 and less than 4 days in the south and the north of Spain, respectively) (Querol et al., 2004a). The MAPAMA (Ministry of Agriculture and Fisheries, Food and Environment) network reported that between 2005 and 2017 there was an average of 14 events of dust intrusion per year that could reach the north of the peninsula. Most of these events are registered in summer and spring (average of 5 per year), with a mean duration of 3 days in both seasons. Winter is the season that registers the fewest number of events (average of 2 per year) with a mean duration of 3 days. Regarding to the Saharan dust intrusions that could reached León between 2005 and 2017, the air quality network of Castilla and León (http://www.medioambiente.jcyl.es/) shows that, approximately, 11% of these events caused an exceedance of the PM_{10} DLV, and on average the PM_{10} levels during the dust outbreaks were between 29 ± 10 μg m^{-3} in summer and 39 ± 13 μg m^{-3} in winter.

There are many studies about the harmful effects of the Saharan intrusions on the Iberian Peninsula, especially in southern cities, but most of them are focused on summer events. However, the studies of winter intrusions and their effects on human health in the north of Spain are scarce. The identification of African events allows determining the contribution of Saharan episodes to the total PM_{10} mass, and the study of these episodes through different disciplines leads to a more comprehensive characterization and a better understanding for the establishment of future mitigation measures. Thus, based on the analyzes of two African dust intrusions in winter 2016 and 2017, which reached the north of Spain, we focus our study on a descriptive understanding of these events including: i) typical synoptic conditions; ii) aerosol chemical composition; iii) particle size distribution; iv) pollen concentration; v) aerosol optical depth; vi) radiative impact and vii) estimation of the impact of aerosols in the respiratory tract.

2. Study area

The study was carried out in León city, Spain, located in the northwest of the Iberian Peninsula, at the University of León (42° 36’ 50” N, 5° 33’ 38” W, 846 m asl) (Fig. 1) in two different periods: i) between 20 and 23 February 2016 and ii) between 21 and 24 February 2017. The city is characterized by the absence of large industries, whilst traffic is considered the main source of particles. The climate in this region is Mediterranean type with continental features, with annual mean temperature of 10.9 °C. Rain events occur irregularly over the year, with minimum precipitation values in summer (80 mm) and maximum values in fall (190 mm). Winters are cold with frequent frosts (74 frost days per year, on average) (Castro et al., 2010).

In February, due to the climatic and floristic characteristics of León city, there are a few pollen types present in the atmosphere, which come from the release of arboreal plants flowering in winter and pre-spring, such as *Alnus, Corylus, Cupressaceae, Fraxinus* and Poaceae (residual). Alder (*Alnus glutinosa*) and hazel (*Corylus avellana*) are part of the natural vegetation of deciduous forest that is about 30 km north of the city. Pollens from these species can be scarce in the atmosphere. The presence of pollen of a large number of species of cypresses and arizonicas (*Cupressaceae*) is very abundant in León, because they are usually used as ornamental trees due to their resistance to extreme climatic conditions. In addition, at the end of February the ash (*Fraxinus excelsior*) pollen begins to appear, which come from the natural vegetation of riverbanks and some parks of León (Oduber et al., 2019).

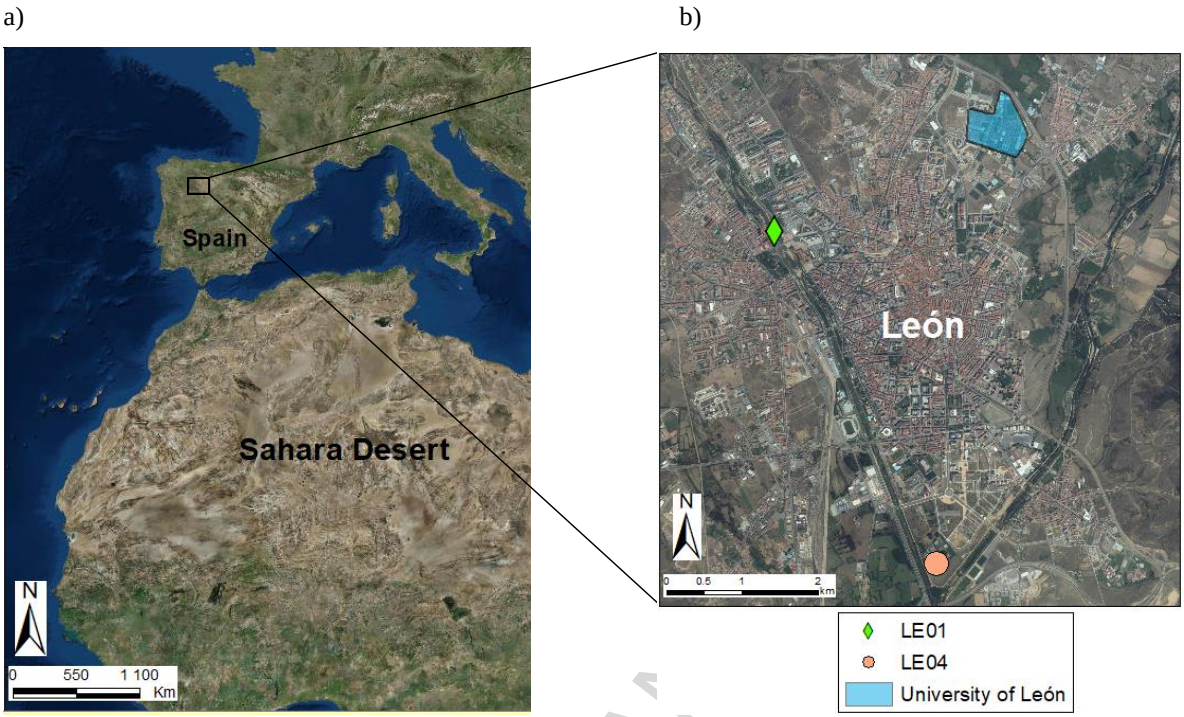

Fig. 1. a) Sahara Desert and region of León (Spain) identified by a black square box; b) León city with the location of the sampling sites and the University of León.

3. Materials and methods

3.1. Sampling instruments

During both sampling campaigns, several continuous measurements were made using different instruments:

- The particle size distributions were measured continuously every minute using a passive cavity aerosol spectrometer probe (PCASP-X, manufactured by Particle Measuring Systems, Inc., PMS) in a range between 0.1 and 10 μm (latex equivalent) in 31 channels. The corrections related to the refractive index and relative humidity were made as explained in previous works (Calvo et al., 2010; Castro et al., 2015, 2018). The accuracy for PCASP measurements is between 16% (concentration) and 20% (diameter) (NOAA, https://www.esrl.noaa.gov). Additionally, a scanning mobility particle sizer (TSI-SMPS Model 3938: DMA 3081 and CPC 3772) for the continuous sampling (on a 6-minute basis) of the submicrometer particles ranging from 14.6 to 791.5 nm, in 112 channels, was used, taking into account the corrections according to Wiedensohler et al. (2012). The uncertainties in the concentration of the measured size distributions are assumed to be 10% from 20 to 200 nm while above this size range it increases to 30% (Wiedensohler et al., 2012).
- Data from an AE-31 aethalometer (Magee Scientific) with a precision of 10^{-3} μg m^{-3} (Blanco-Alegre et al., 2019) were used to estimate the iron content from aerosol dust (on a 2-minute basis) by the two component model

detailed in Fialho et al. (2006). The load correction model proposed by Weingartner et al. (2003) was used. Considering scattering measurements were not available for the experiment, the best approximation for Weingartner et al. (2003) *f* (describing the shadowing effect) were taken from the winter values proposed in Sandradewi et al. (2008).

- For pollen monitoring, a volumetric Hirst-type spore-trap (Lanzoni VPPS 2000) was used. Daily and hourly pollen counts were made using optical microscopy for the identification of pollen and spores, following the method recommended by the Spanish Aerobiological Network and fulfilling the aerobiological quality requirements of the European Aerobiology Society (Galán Soldevilla et al., 2007). The estimated uncertainties associate with the pollen measured, with the working conditions, was about 10% (Oteros et al., 2017; UNI 11108:2004, 2004).

Furthermore, for the event of 2016 the optical properties of aerosols along the atmospheric vertical path, were measured with a Cimel CE318 Sun/Sky Photometer. The calibration of the direct component was performed using the Langley method during a period with stable and low atmospheric turbidity conditions. The irradiance calibration uncertainty is 1-2%, depending on the channel (Holben et al., 1998). The aerosol optical depth (AOD) was retrieved by ESR.PACK code, which is based on the SKYRAD.PACK algorithm (Takamura and Nakajima, 2004). The AOD retrieved by ESR.PACK is comparable to the retrieval of the Aerosol Robotic Network (AERONET) of NASA, with mean deviation values between -0.0030 and +0.0041 (0.012 in the case of AOD at 340 nm) (Estellés et al., 2012). Absolute error for AOD retrieval with the Cimel sun photometer within AERONET protocols is 0.01-0.02 (Holben et al., 1998). The Ångström exponent (AE, dimensionless), as indicator of the average particle size, was calculated using AOD at 440 and 870 nm.

During the event of February 2017, three simultaneous 24 h samplings of PM_{10} were carried out, starting at 1200 UTC. Two of them, by means of two low volume samplers, TECORA ECHOPM operated with 47 mm diameter teflon filters and a Gent PM_{10} stacked filter unit sampler operating with 47 mm diameter polycarbonate filters (0.2 µm pore size). The third sample was taken by a high-volume sampler (CAV-A/Mb) equipped with a 150 mm diameter quartz filter. The dates of the filters refer to the beginning of the sampling (from 1200 UTC of that day to 1200 UTC of the next day).

3.2. Analytical methodologies

Quartz filters were used for the quantification of PM_{10} by gravimetry using an electronic microbalance (Mettler Toledo, XPE105DR) and for the determination of organic and elemental carbon (OC and EC, respectively) by a thermo-optical technique developed by the University of Aveiro, Portugal (Alves et al., 2015; Pio et al., 2011). The calculated uncertainties on concentrations measured by this analytical method ranged between 5-10%.

The quantification of water-soluble inorganic ions (Na^+, K^+, Ca^{2+}, Mg^{2+}, NH_4^+, Cl^-, SO_4^{2-}, NO_3^- and NO_2^-) was carried out using the solution obtained after extraction of teflon half filters with 6 mL of ultra-pure deionized water, and subsequently analyzed in a Thermo Scientific Dionex™ ICS-5000 Ion Chromatograph. The other half of the teflon

filters were used for the determination of the major trace elements by PIXE (Particle-Induced X-ray Emission), following the methodology described by Lucarelli et al. (2015). The estimated uncertainties for the ion chromatography and PIXE measurements are dependent on the analysed element and their limits of detection. These uncertainties can ranged from 2% to 20% in PIXE and between 5-10% in ion chromatography (Lucarelli et al., 2015).

The morphology and elemental composition of individual aerosol particles collected on the polycarbonate filters were investigated by Field Emission Scanning Electron Microscopy (FE-SEM) using a Tabletop Microscope Hitachi TM-100 and a Digital Scanning Microscope DSM950.

3.3. Additional databases and statistical treatment

Additional data (PM_{10} and SO_2) from two air quality stations belonging to the regional air quality network (http://www.medioambiente.jcyl.es/) were used: the urban traffic station LE01 is located in an urban residential area in San Ignacio de Loyola Avenue (05° 35'14"W 42° 36'14"N) and the suburban/background station LE04, located in Coto escolar (05° 33'59"W 42° 34'31"N) (Fig.1), which is not directly influenced by vehicular, industrial or residential emissions. The data were recorded from 0000 UTC of the sampling day to 0000 UTC of the next day.

Furthermore, meteorological parameters such as temperature, relative humidity, precipitation, wind speed and direction were recorded by an automatic weather station located in the sampling site.

The origin of air masses during the study period was interpreted by the determination of daily 3-day back trajectories (at 500, 1500 and 3000 m agl) using the HYSPLIT model (Draxler and Rolph, 2012; Rolph et al., 2017; Stein et al., 2015). The Spanish Meteorological Agency (AEMET) provided visibility and diffuse and direct radiation data for the studied period.

The statistical treatment has been carried out using the SPSS software (IBM Statistics Software V. 24). The correlation between pollutant concentrations was made using the nonparametric Pearson correlation method. The Kruskal-Wallis non-parametric test (Kruskal and Wallis, 1952), followed by the Dunn 1964 test, was applied to the data in order to find statistically significant differences.

3.4. Estimation of the aerosol clear sky radiative forcing

The aerosol clear sky radiative forcing has been estimated using the discrete ordinate Radiative Transfer Model Global Atmospheric ModEl (RTM GAME) (Dubuisson et al., 2004, 1996). Upward and downward net radiative fluxes are calculated over the entire short-wave region and are performed at every 3 h interval and for the whole study period with and without aerosols. From these fluxes, we computed the aerosol clear sky daily direct forcing at the bottom of atmosphere (ΔF_{BOA}) and at the top of the atmosphere (ΔF_{TOA} - 20 km in this case). With the considered convention here, a positive sign of ΔF_{BOA} and ΔF_{TOA} indicates an aerosol warming effect. The atmospheric forcing ΔF_{ATM} was estimated through the difference between the top and bottom aerosol direct forcing; it represents the possible absorption of solar radiation due to absorbing particles within the atmospheric specified aerosol layers. An important point for

estimating the direct forcing of aerosols is their vertical profile within the atmosphere and associated optical properties. The single scattering albedo (*SSA*), asymmetry parameter (*g*) and extinction coefficient profiles were also determined with the same methodology as described by Calvo et al., (2010). Vertical profiles of atmospheric properties such as relative humidity, temperature, pressure and ozone concentrations have been measured through radiosoundings available at National Oceanic and Atmospheric Administration (NOAA) for the whole study period.

3.5. Estimation of the health impacts: particles deposition in respiratory tract regions

Following the Spanish standard UNE (1997) (equivalent to ISO, 1995), the aerosol size fractions deposited in respiratory tract regions (inhalable, thoracic, tracheobronchial and respirable) were estimated considering the following parameters: i) the number of particles in each channel of the PCASP-X and SMPS; ii) the aerodynamic diameter corresponding to these channels and iii) the estimated aerosol density (Alonso-Blanco et al., 2018; Castro et al., 2015, 2018; Morawska and Salthammer, 2003).

4. Results and discussions

4.1. Synoptic conditions and meteorological considerations

On 19 February 2016, the anticyclone of the Azores extended its influence on the Iberian Peninsula, with isobars up to 1028 hPa on the area of study. The peninsular south started to be affected by the relative low pressures from North Africa. At 500 hPa (charts not shown here), a trough centered on the peninsula was observed. On 20 February (Fig. 2a) African air continued entering the peninsular south, both at ground (isobars of 1024 hPa) and at 500 hPa, and there was a parcel of colder air coming from the rupture of the previous day trough. The Atlantic anticyclone influenced the rest of the Peninsula with a center of high pressure (1032 hPa) very close to the study area. This center was intensified (up to 1034 hPa) and moved towards northeast on the next day, allowing the mass of African air to advance from the south, and reaching the peninsular latitude. At 500 hPa level, the air parcel located in the NE of the Canary Islands favored this African air intake.

The surface map on 22 February 2016 (Fig. 2b), presents the temporary retreat of the Atlantic anticyclone, together with the connection of a center of high pressures on the Northern Peninsula with a center of relative low-pressure placed on the Gulf of Cadiz. The same situation is observed at 500 hPa. As a result, African air continued entering directly into Iberia and towards higher latitudes. Finally, from 23 February, the peninsular high-pressure system moved towards the south, up to the north of Africa, and the influence of the Azores Anticyclone affected again to the whole Peninsula, causing winds from north or northeast that opposed the entry of African air, hence the disappearance of the air parcel located to the SW of the Peninsula.

a) b)

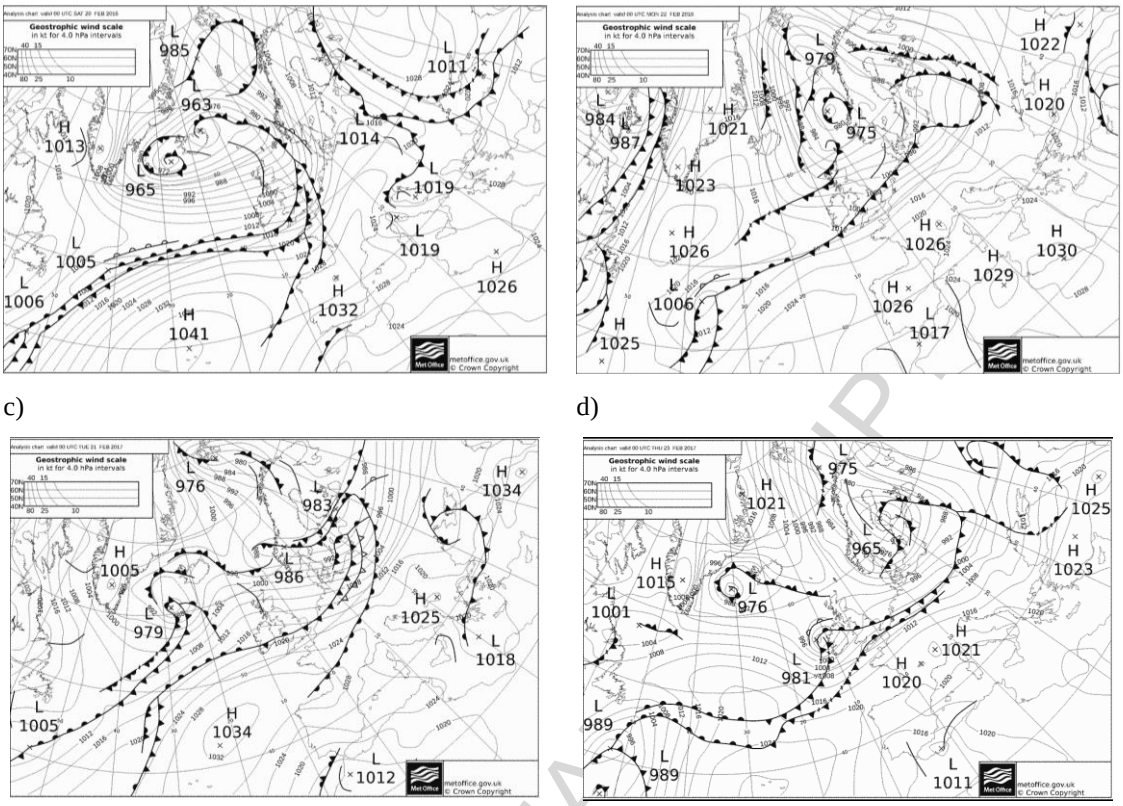

Fig. 2. Synoptic charts (surface pressure) for 20 and 22 February 2016 a) and b), 21 and 23 February 2017 c) and d).

On 21 February 2017 (Fig. 2c) a clear influence of the anticyclone of the Azores on the northern half of the peninsula was observed, while the southern half became affected by the airflow caused by the low pressures located to the north of Africa, which is also observed at 500 hPa level (chart not shown here). This situation remained almost unchanged in the surface chart of the next day, although the anticyclonic influence had weakened, and the relative low-pressure system had moved towards the Gulf of Cadiz, thus maintaining the entry of African air into the peninsular South.

The isobaric configuration of Thursday, 23 February 2017 (Fig. 2d), evidences the rupture of the anticyclonic influence as a result of a barometric swamp (or flat low) located in the peninsular North that facilitated the movement of the Saharan air towards higher latitudes, pushed by the air movement around the low of the North African. Therefore, the airflow from North Africa continued both in surface and in height. Nevertheless, this lack of definition in the isobars did not last long: the day after, the Atlantic anticyclone advanced on the Bay of Biscay and the anticyclonic influence returned to the peninsula, with wind flow from northeast. Simultaneously, a cold front advanced from north, resulting in a change in the air mass arriving to the study area. This situation became stable on the following day, when an anticyclone center appeared on the Bay of Biscay, with a wide influence over the entire Iberian Peninsula, thus preventing the entrance of African air from south.

The HYSPLIT model allows evidencing the arrival of air masses coming from North Africa in both events (Fig. 3) and the NAAPs model shows the dust load over Iberia on 22 February 2016 (Fig. 3c) and 23 February 2017 (Fig. 3d). Furthermore, an increase in the temperature and a decrease in the relative humidity, on 22 February 2016 (+1 °C and -10 %, respectively) and on 23 February 2017 (+3 °C and -23 %, respectively), were registered. The meteorological data recorded at the sampling point showed that the mean temperature and relative humidity for February 2016 and 2017 in León were 5 ± 4 ºC and 76 ± 16 %, respectively.

4.2. Impact on particulate matter

4.2.1. PM_{10}

Over the course of 21 and 22 February 2016, a progressive increase in the PM_{10} concentration was observed in the stations LE01 and LE04, reaching the maximum hourly value on 22 February between 1200 and 1400 UTC, with 113 µg m^{-3} and 75 µg m^{-3}, for the stations LE01 and LE04, respectively. The DLV was exceeded on 22 February 2016 (daily mean of 52 µg m^{-3} in station LE01). The Kruskal-Wallis test (Kruskal and Wallis, 1952) shows that there were significant differences ($p< 0.05$) between mean PM_{10} values in the previous days (mean hourly concentration between 20 at 0000 UTC and 21 at 0800 UTC of 22 ± 18 µg m^{-3}) and during (mean hourly concentration between 21 at 0900 UTC and 23 at 0900 UTC of 41 ± 27 µg m^{-3}) the Saharan dust intrusion. This unusual episode was also studied by Titos et al. (2017) in Northeastern Spain. They reported an exceedance of PM_{10} DLV in 90% of the 250 air quality stations across Iberia and Balearic Islands on 22 February, as in this work. Also, from the gravimetric analysis of 24 h filter, they registered a PM_{10} mass concentration of 97 µg m^{-3} on 23 February 2016 in Montsec, in the NE of the peninsula, and found that 80% of the PM_{10} mass was from mineral origin.

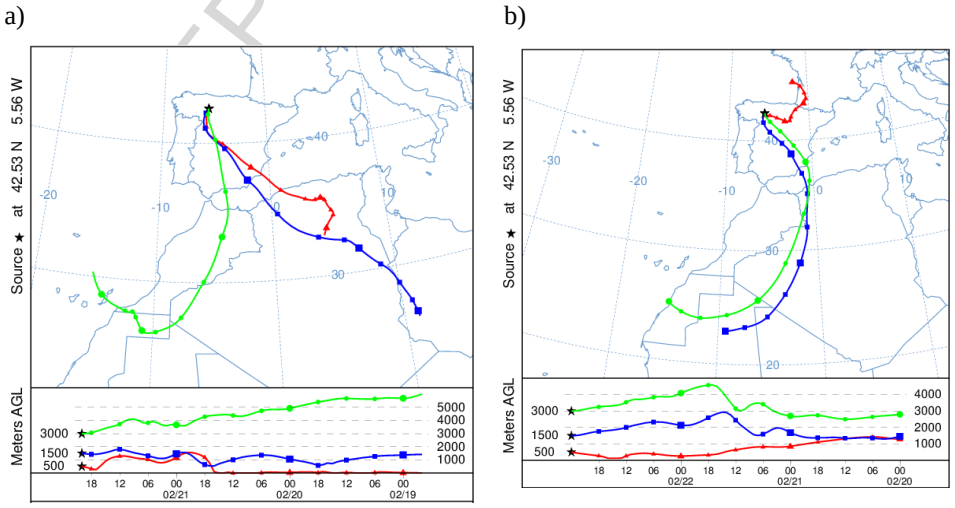

c) d)

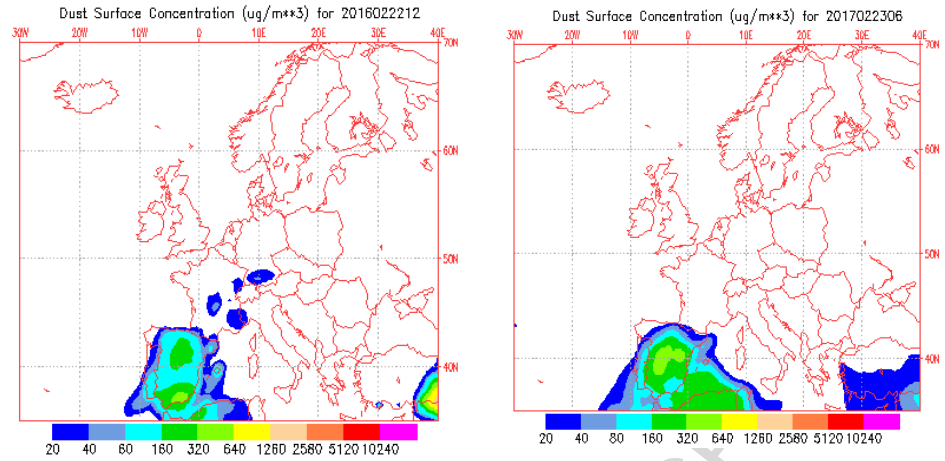

Fig. 3. a) HYSPLIT back trajectories at 500, 1500 and 3000 m agl on a) 22 February 2016 at 2000 UTC and c) 21 February 2017 at 0000 UTC, and NAAPs images of dust concentration on c) 22 February 2016 at 1200 UTC and d) 23 February 2017 at 0600 UTC.

Regarding the dust intrusion event of February 2017, an increase in the PM_{10} level was observed between 22 February at 2000 UTC and 24 February 2017 at 0900 UTC in both air quality stations, LE01 and LE04 (Fig. 4), reaching a maximum value of 156 µg m^{-3} on 23 February at 1200 UTC (data from station LE01). On 23 February, the PM_{10} DLV was exceeded (daily mean 86 µg m^{-3} were recorded at station LE01). This concentration was more than three times the value measured in days without intrusion (26 ± 14 µg m^{-3}). The Kruskal and Wallis test showed significant differences ($p< 0.05$) between PM_{10} values in days before and during the Saharan dust intrusion.

On 20 February 2016, and 21 February 2017, before the Saharan dust plumes reached León city, important increases in PM_{10}, accompanied by an increase in the SO_2 concentrations (Fig. 4a and 4c), were observed. However, these peaks were not registered by the station LE04 (Fig. 4b and 4d). The station LE01 is located in an urban area, where the emissions from traffic and domestic heating devices (including coal combustion appliances, emitting SO_2) are important and can trigger the PM_{10} levels causing the exceedance of the DLV.

a)

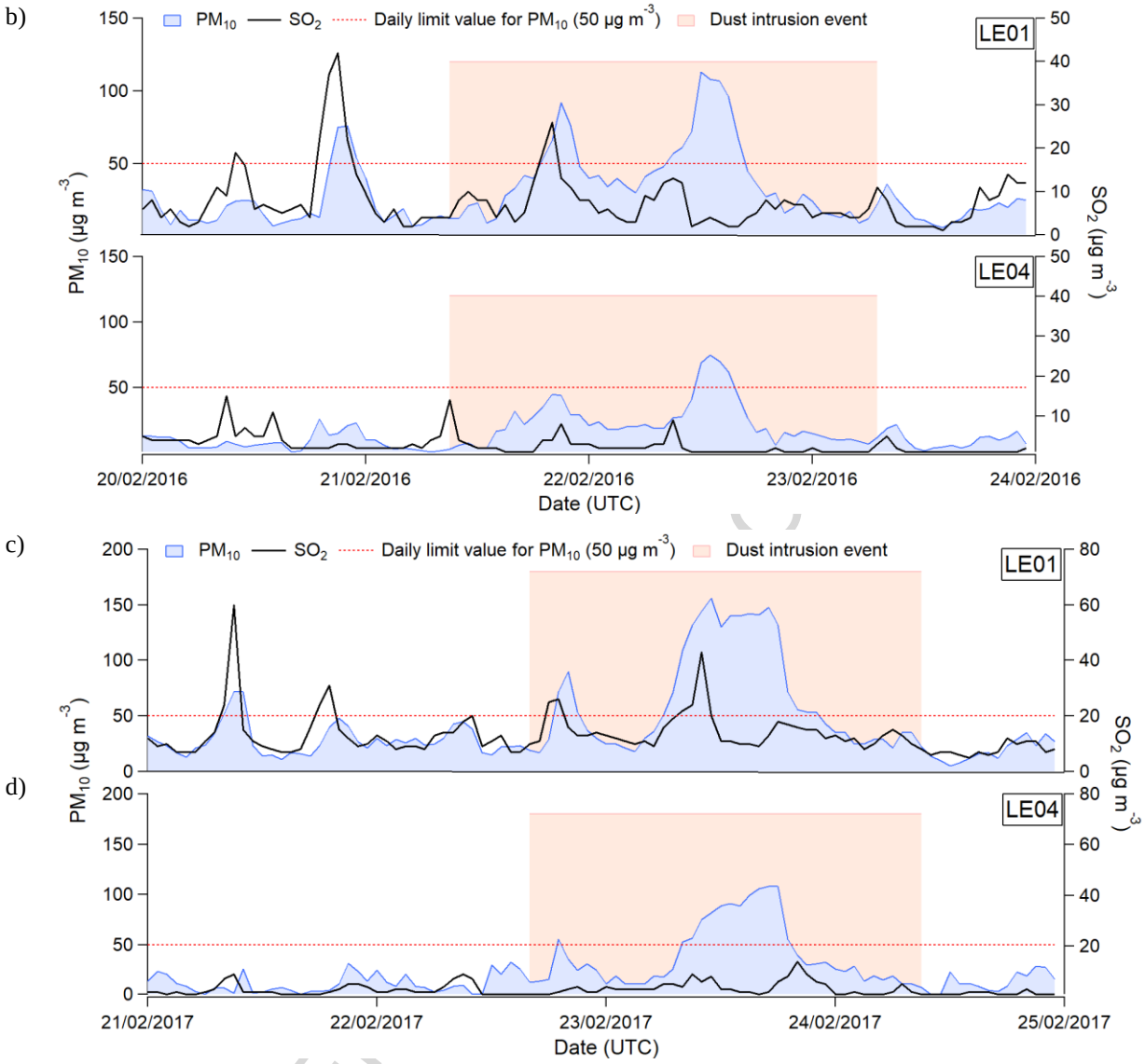

Fig. 4. Hourly evolution of PM_{10} and SO_2 during the 2016 and 2017 Saharan dust outbreaks at LE01 [a) and c)] and LE04 [b) and d)].

Due to the particularity of both studied events, and in order to establish the differences and similarities between those and other dust events that reached the Iberian Peninsula, a brief comparison and analysis has been carried out in this section. Table 1 shows several dust episodes, which may have affected the air quality of different cities in Spain.

Table 1. Maximum PM_{10} concentration and duration in days of different Saharan dust events that affected the Iberian Peninsula.

Reference	Study zone	Station	Study period	Season	Duration (days)	PM_{10} (µg m^{-3})

This work (PM_{10} data from air quality network)	León (NW)	Urban, traffic	20-24 February 2016	Winter	2	52
			21-25 February 2017		1	86
PM_{10} data from air quality network	León (NW)	Urban, traffic	21 March 2014	Spring	1	**21**
			12-17 April 2015		5	51
			29-30 August 2015	Summer	2	**31**
			19-20 July 2016		2	**43**
			26-27 August 2017		1	**38**
Escudero et al. (2007)	Peñausende (NW)	Background	21-29 March 2002	Spring	3	62
	O Saviñao (NW)					88
			16-28 June 2003	Summer	4	**43**
Rodríguez et al. (2001)	Carboneras (SE)	Rural	22- 23 January 1997	Winter	2	147
	Monagrega (NE)	Rural	4-5 June 1998	Summer	2	71
Nicolás et al. (2008)	Elche (SE)	Urban, background	16 July 2005	Summer	1	58
Titos et al. (2017)	Southwest		20-25 February 2016	Winter	2	> 200
	Southeast					> 150
	East					> 50
	Centre					> 150
	North					< **50**
	Northeast					> 50
Cachorro et al. (2008)	Peñasuende (N)	Background	22 July- 3 August 2004	Summer	5	200
	Campisablos (Centre)					100
Coz et al. (2010)	Casa de Campo, Madrid (Centre)	Suburban	16 March 2004	Spring		98
	CIEMAT, Madrid (Centre)	Suburban background				92
Artíñano et al. (2003)	Escuelas Aguirre, Madrid (Centre)	Urban	29 June- 2 July 1999	Summer	3	63
			11-12 July 1999		2	53
			24-26 July 1999		3	63
			19 August 1999		1	54
			24-25 August 1999		2	80
			27-29 October 1999	Autumn	3	88
			5-13 March 2000	Spring	8	70
			15-17 May 2000		3	**47**

As observed in Table 1, the PM_{10} DLV is not usually exceeded during intrusion events in the city of León. This fact gives more importance to the extremely unusual behavior observed during the dusty period of February 2016 and 2017, which reached PM_{10} values even more higher than those observed in summer or spring Saharan outbreaks in this city. The intrusion event of 2017 also showed a higher intensity compared with that of 2016, showing a PM_{10} similar to that reported by Artíñano et al. (2003), Escudero et al. (2007) and Rodríguez et al. (2001) during summer and spring dust intrusions. Due to the proximity of the dust source, southern regions of Spain are more affected than northern regions by dust outbreaks (about 200 km and 800 km far from North Africa, respectively), as observed by Rodríguez et al. (2001) and Titos et al. (2017), who reported values of PM_{10} higher than 100 μg m^{-3} in different winter Saharan

dust intrusions in contrast with those observed in northern locations were the PM_{10} levels do not reach such concentration.

4.2.2. OC and EC

The evolution of the carbonaceous fraction before and during Saharan dust intrusions of 2017, is not well defined. Taken into account the quartz filters samples between 18 and 21 February as before the intrusion, and between 23 and 24 as during the Saharan dust intrusion, the following results were observed: the carbonaceous (OC + EC) fraction barely change during the dust intrusion, going from 16 ± 4 % between to 8 % of PM_{10} mass; organic carbon (OC) concentration slightly increase during the intrusion, from mean concentrations of 2.3 ± 0.6 and 4.2 μg m^{-3}, before and during the dust event, respectively; elemental carbon (EC) concentration do not show a significant change during the Saharan intrusion (0.7 ± 0.3 and 0.8 μg m^{-3} in days without and with Saharan dust outbreaks, respectively). Some authors as Aymoz et al. (2004) and Putaud et al., (2000) reported an increase in the OC concentration associated with mineral dust, during summer Saharan dust outbreaks in France in 2000 and Tenerife Island in 1997, respectively. This increase is probably due to the contribution of hundreds of organic compounds transported during these events. The low variability of EC concentration during the dust outbreak, may indicate that the dust cloud was not mixed with anthropogenic sources during the transport (Fig. 3), which could have caused an increase in EC concentrations. Thus, the EC signature is linked to local sources influence.

4.2.3. Trace elements

The chemical composition of the 24 h teflon filters, sampled during the intrusion, between 23 and 24 February, shows that the increase in the PM_{10} mass concentrations was due to an increase in the mass concentration of Al, Ca, Si, Fe, Mg and Ti (Table 2). These elements are generally associated with a crustal source (Alastuey et al., 2016; Aymoz et al., 2004; Caquineau et al., 1998; Viana et al., 2002). The statistically significant correlation between PM_{10} and each crustal element (r = 0.9, p< 0.01), confirmed the important contribution from crustal material to PM_{10}. Si, Ca, Al, Fe and Mg represent up to 5.5% of the PM_{10} during the dust intrusion, while on the remaining days, the contribution did not reach 3% of the PM_{10} mass. This behavior was also reported by Viana et al., (2002) for winter intrusion events in the Canary Islands, located west of the Saharan Desert, between 1998 and 2000, with a significant increase in the Si, Al, K, Ti, Ca, Fe, Mn, Mg and Ba concentrations.

Table 2. Mass ratio (element/PM_{10}) (%) and mean concentration (mean ± standard deviation) for the crustal elements present in the four filters sampled between 18 and 22 February (before the Saharan dust) and in the filter sampled during the Saharan dust event (23 February 2017).

	% of PM_{10} mass		**Concentration (μg m^{-3})**	
	Before	**During**	**Before**	**During**
PM_{10}			19 ± 3	59
Al	0.5 ± 0.2	5.6	0.10 ± 0.04	3.31
Ca	1.0 ± 0.5	3.4	0.20 ± 0.10	2.04
Si	1.3 ± 0.6	11.1	0.25 ± 0.11	6.53

Fe	0.9 ± 0.4	3.3	0.18 ± 0.07	1.96
K	0.7 ± 0.2	1.4	0.13 ± 0.03	0.852
Mg	0.12 ± 0.04	1.05	0.022 ± 0.008	0.619
Mn	0.015 ± 0.006	0.054	0.0028 ± 0.0010	0.0316
Na	0.8 ± 0.3	0.6	0.16 ± 0.06	0.36
Ti	0.04 ± 0.02	0.34	0.008 ± 0.004	0.204

a)

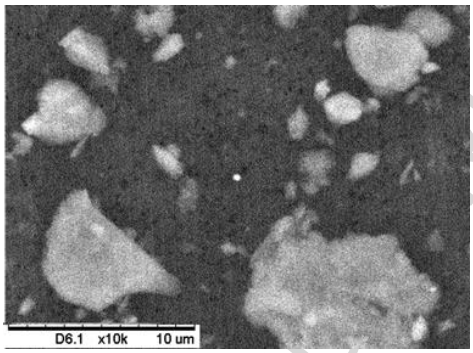

b)

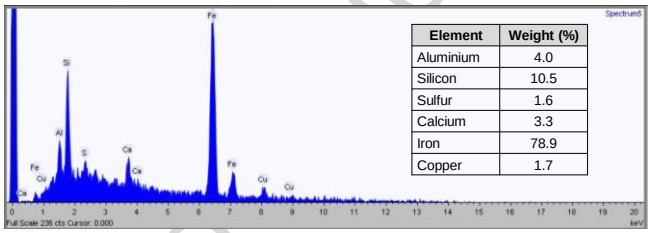

Fig. 5. a) SEM image and b) elemental composition of individual aerosol particles collected on the polycarbonate filter on 23 February to the 24 February 2017.

The total mineral fraction (∑ Al_2O_3, SiO_2, Ca, Mg, Fe and K) represents 44% of the PM_{10} mass during the dust outbreak and only 7% for the period before the outbreak. The SEM analysis also showed the presence of coarse particles mainly with Si, Al and Fe composition (Fig. 5). The mineral mass concentration reached 27 µg m^{-3} during the Saharan dust intrusion versus 3.2 µg m^{-3} and 2.2 µg m^{-3} registered days before and after the event, respectively. These results are coincident with the typical levels of mineral dust reported by other authors in Spain. In a study conducted in Elche, Spain, between 2004 and 2005, Nicolás et al. (2008) showed that the mean African dust contribution to PM_{10} mass concentration during normal days were 3.3 and 1.2 µg m^{-3} in summer and winter, respectively. Querol et al. (2004b), in a study carried out in the Iberian Peninsula between 1998 and 2002, reported that the mean mineral contribution to PM_{10} ranged between 5.5 and 2 µg m^{-3} in the south and east, and in the remaining areas, respectively. Additionally, Viana et al. (2014) showed that, in Spain, in 2008 and 2009, the main source of natural aerosol was African dust, even more than sea spray, and the contributions of mineral source to PM_{10} levels in 2008 and 2009, ranged between 1 and 4 µg m^{-3} from north to south, through the year. Alastuey et al. (2016) reported higher concentrations of mineral dust in summer compared to winter (up to 10 µg m^{-3} and less than 2 µg m^{-3}, respectively) in

a study carried out in several European cities between 2012 and 2013, due to the high frequency of dust events during summer.

4.2.4. Water soluble inorganic ions

An increase in the SO_4^{2-}, Cl^- and NO_3^- concentrations associated with the increase of PM_{10} concentration was also observed (Fig. 6). Dentener et al. (1996) and Liao (2003) showed that, in areas close to the source regions of mineral dust, sulfate and nitrate can be associated with the coarse mode of the aerosol. Galindo et al. (2008) also reported an increase in sulfate and nitrate concentrations in coarse size fractions in a study carried out in southern Spain between 2003 and 2004, during summer Saharan dust outbreaks, compared to normal days.

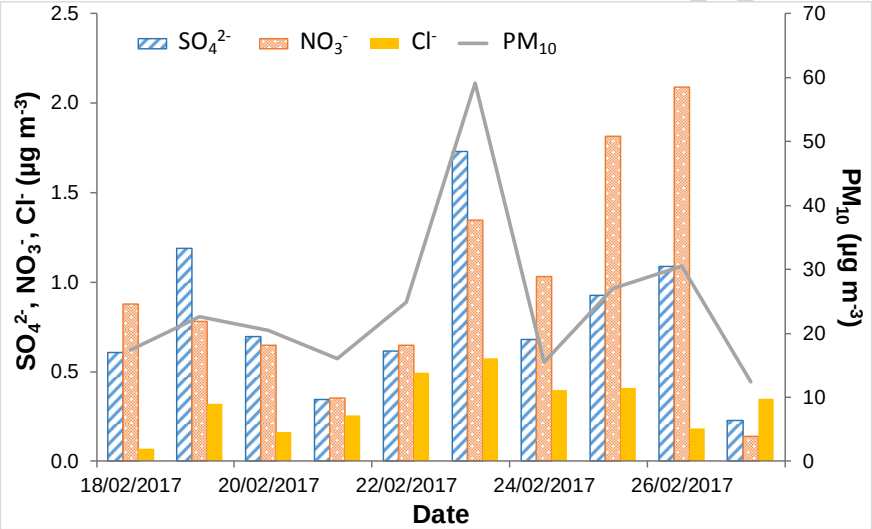

Fig. 6. Daily evolution of SO_4^{2-}, NO_3^-, Cl^- and PM_{10} concentrations during the intrusion of February 2017.

The SO_4^{2-}/Ca^{2+} mass ratio on 23 February to 24 February 2017 was 1.4, while for previous (between 18 and 21) and subsequent days (between 24 and 28) the mean value was 3.9 ± 1.4. Putaud et al. (2000) reported a SO_4^{2-}/Ca^{2+} mass ratio between 1.8 and 2.9 for Tenerife Island (Spain) during a Saharan outbreak in summer 1997. They also suggested that a pure Saharan dust mass ratio should be about 0.4-0.6, according to the ion chromatographic analysis carried out on samples of fine grains of sand from the Sahara Desert. The difference observed between the pure dust mass ratio and our results could be attributable to the contribution from anthropogenic sources that could increase the SO_4^{2-} levels. Moreover, the Cl^-/Na^+ ratio obtained during the dust outbreak was 1.6, while in days before and after the event the mean value was 1.3 ± 0.3. These relationships are very close to the one reported by Aymoz et al. (2004) for halite (1.5), which suggests an enrichment of the mineral fraction of the aerosol during the dust outbreaks.

4.2.5. Estimation of iron concentration from aethalometer data

The time series of the aethalometer data for black carbon (BC) and the estimated iron dust after the application of two component model (Fialho et al., 2006, 2014) is consistent with the presence of high quantities of dust during

Saharan intrusions. Figure 7a shows a first peak on 20 February 2016. As mentioned in the previous section, this peak registered before the intrusion is probably due to a local pollution episode related to coal combustion and/or biomass burning. The emission of brown carbon (BrC, light-absorbing organic carbon) during these activities (Bond, 2001; Olson et al., 2015; Yang et al., 2009) enhances the aethalometer attenuation signal (Fialho et al., 2014), giving rise to a "false Fe peak". When the Saharan dust plume reached León on 21 February, an increase in the iron concentration was observed, reaching a maximum of 4.1 µg m^{-3} and a mean value of 0.8 ± 0.7 µg m^{-3} during the dusty period between 0900 UTC 21 and 0900 UTC 23, while before and after the event (between 0000 UTC 21 and 0800 UTC 21, and between 1000 UTC 23 and 0000 UTC 24, respectively), the mean iron value was 0.7 ± 0.7 µg m^{-3}, confirming the high contribution from this natural source during the outbreak (Guerzoni et al., 1997; Guieu et al., 2002).

On 23 February 2017, an important increase in both black carbon and iron concentrations is also observed (Fig. 7b), reaching a maximum value of Fe on 23 February at 10:16 (UTC) of 5.3 µg m^{-3}. The Fe concentration estimated by the aethalometer during the Saharan dust outbreak (23 to 24 February 2017) was 1.3 ± 0.8 µg m^{-3}. The value obtained from PIXE for one-day sampled filter during the same period was 2.0 µg m^{-3}, which falls within the aethalometer results range.

a)

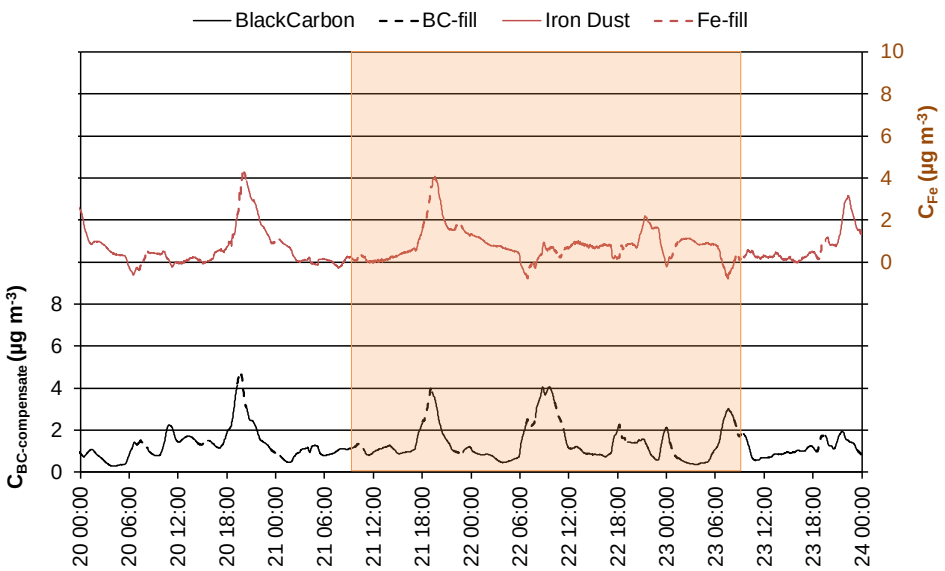

b)

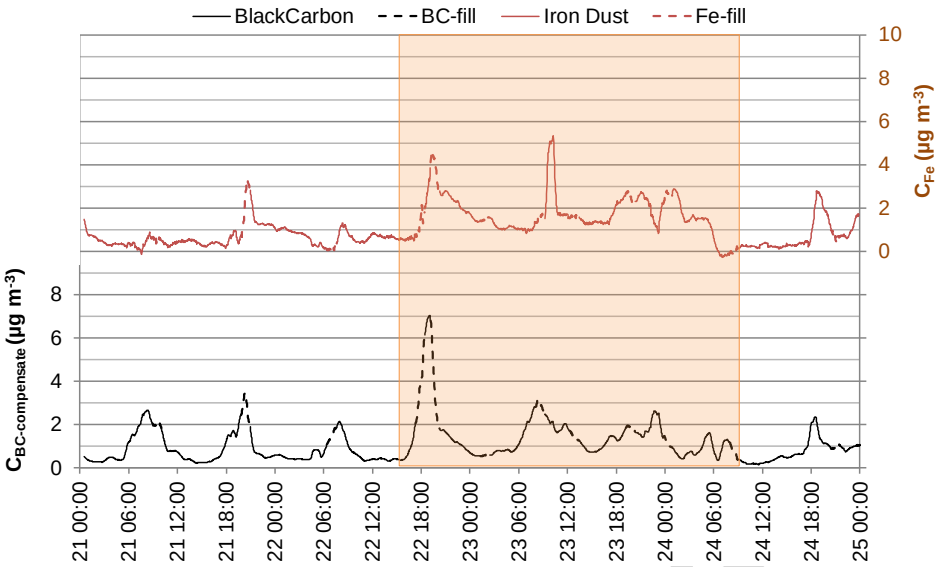

Fig. 7. Two-minute moving average of iron dust (red) and black carbon (black) concentrations between a) 20 and 24 February 2016 and b) 21 and 25 February 2017. The orange shadow shows the dust intrusion period.

4.2.6. Aerosol size distribution

The evolution of the aerosol size distributions, total particle number concentration (N_t) and particles concentration belonging to each of the three modes (nucleation, Aitken and accumulation) was also investigated through the data obtained from the PCASP and SMPS. The corrections corresponding to the data from the PCASP were carried out using a refractive index and a density for the days without intrusions (1.645 – 0.01016*i* and 2.086 g cm^{-3}, respectively) and for the days with intrusion (1.601 – 0.00755*i* and 2.295 g cm^{-3}, respectively), which were calculated from aerosol composition described by Alves et al. (2014), following the methodology described by Levin et al. (2010). Figure 8a shows a first peak in the particle number concentrations of the three modes (nucleation, Aitken and accumulation) at 1900 UTC on 20 February 2016 (37 × 10^3 particles cm^{-3}), with maxima in the aerodynamic diameter interval 30-100 nm, suggesting emissions from anthropogenic sources (Charron and Harrison, 2003; Wehner and Wiedensohler, 2002) and confirming the contribution from domestic heating devices and traffic observed in Figure 4a. Dust intrusion events were evidenced by the increase in the total particle number concentrations, reaching a maximum of 25 × 10^3 particles cm^{-3} on 21 February 2016 at 1900 UTC (Fig. 8a) and 11 × 10^3 particles cm^{-3} on 22 February 2017 at 1900 UTC (Fig. 8b). Additionally, there was an important increase of particles with aerodynamic diameters > 100 nm, reaching the maximum of 3.9 × 10^3 particles cm^{-3} on 22 February 2016 and 4.4 × 10^3 particles cm^{-3} on 23 February 2017.

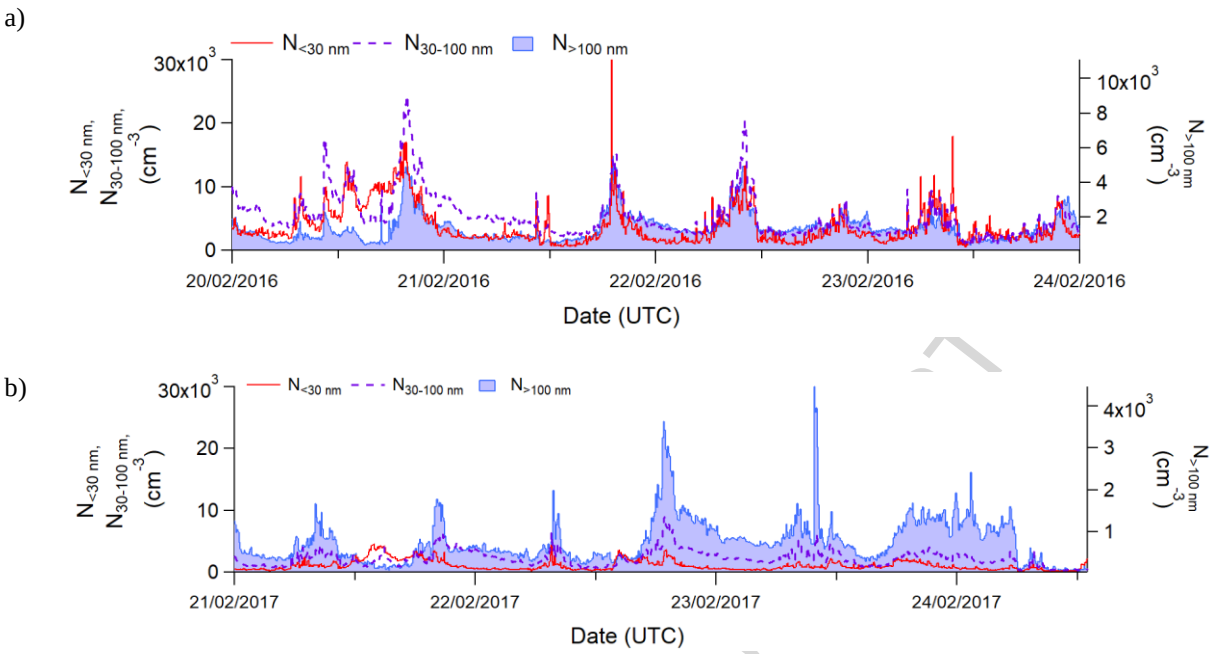

Fig. 8. Evolution of the aerosol size distributions and particles concentration for each of the three modes: nucleation ($N_{<30\ nm}$), Aitken ($N_{30\text{-}100\ nm}$) and accumulation ($N_{>100\ nm}$) during the study period of a) 2016 and b) 2017.

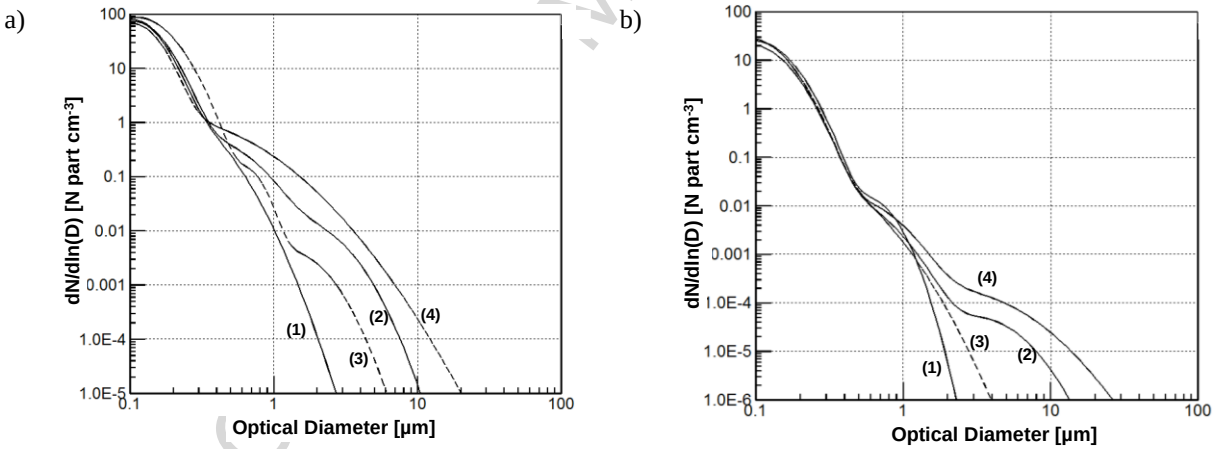

Fig. 9. Theoretical aerosol size number for the intrusion of 2016 (a), and for 2017 (b). The lines corresponding to days before (1), during (2) and after (3) of the intrusion, and the time when the maximum PM_{10} level was reached (4) during the intrusion.

The day before the Saharan dust intrusion of 2016, the particle size distribution showed a unimodal profile (Fig. 9a), with one fine mode (~ 0.1 µm), which indicates a contribution from road traffic (Calvo et al., 2013). When the dust plumes arrived in León, a small fraction corresponding to a coarse mode (~2 µm) confirmed the presence of dust particles (Ansmann et al., 2003; Córdoba-Jabonero et al., 2011; Struckmeier et al., 2016). This behavior was also

detected by Titos et al. (2017). They reported the existence of a coarse mode (~ 3 µm) during their study of the event of February 2016 in Montsec, Spain. Moreover, before the dust event of 2017, a bimodal profile was observed (Fig. 9b) with modal diameter of the number size distribution at about 0.1 and 0.6 µm, indicating the contribution of anthropogenic sources. On 23 February 2017 a small fraction corresponding to a coarse mode (particle diameter D_p ~ 3 µm) attributable to dust particles (Denjean et al., 2016) was registered, which was also recorded the next day. The high concentration of coarse particles during the event of 2017 was confirmed by the morphological analysis. Thus, Figure 10 shows a high number of particles larger than 1 µm on 23 February 2017, compared with the filter sampled on 23 March 2017 (day without dust intrusion) in León.

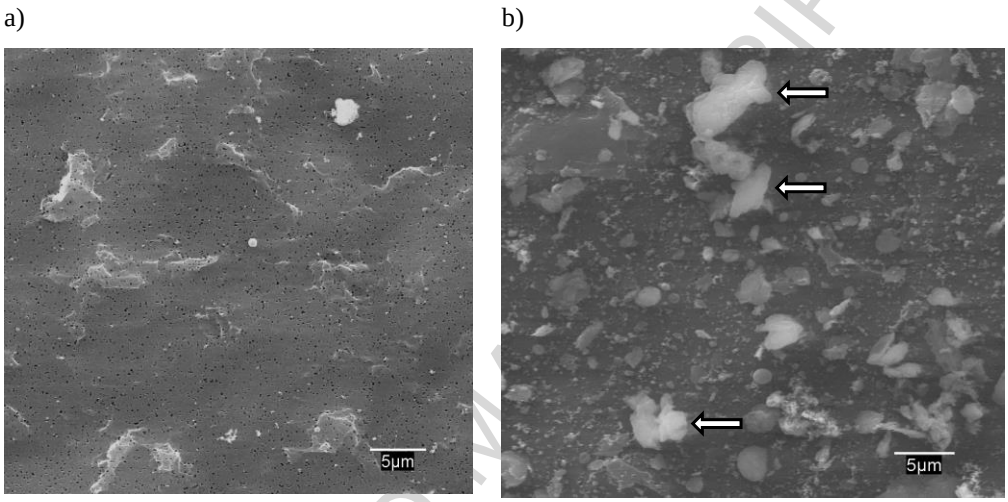

Fig. 10. SEM images of a) day without Saharan dust intrusion and b) on 23 February, 2017. The withe arrows point to some of the dust particles.

4.3. Impact on columnar properties

4.3.1. Optical depth

Following the information of the temporal evolution of the aerosol optical depth (AOD) and the Ångström exponent (AE) over León, the intensity of the desert dust outbreak of the event of 2016 was quantified. The criteria conditions used for dusty and background conditions at León during this episode are the following: low AOD≤ 0.1 and high AE ≥1 correspond to background conditions, a Saharan dust episode is detected with values of high AOD and low AE≤ 0.5, and periods of transition between these two patterns are characterized by moderate AOD and 0.5≤ AE≤ 1. The rapid arrival of the desert dust plume is observed with the increase of AOD and the decrease of AE during the early morning of 21 February. The following day, 22 February, shows a clear desert aerosol character, registering at

0950 UTC the highest AOD with a value of 1.1 and the lowest AE with 0.05. The desert dust aerosol quickly moved away, which dropped back to background levels on 23 February, confirming the results previously analyzed (Fig. 11).

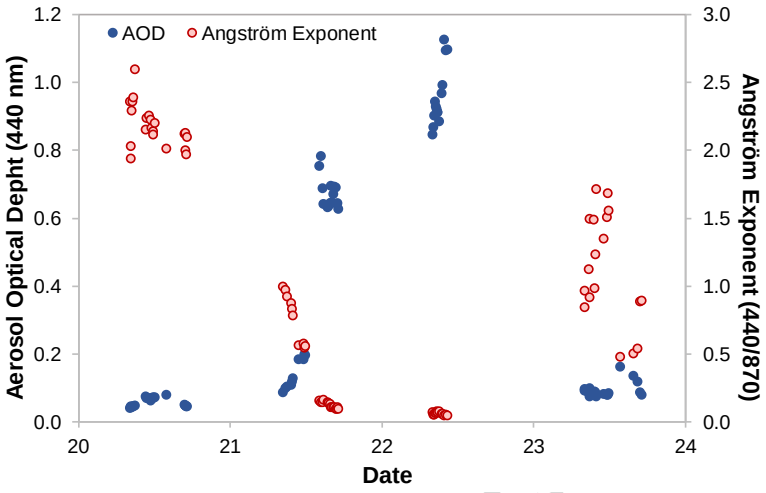

Fig. 11. Time series of AOD (440 nm) and Ångström exponent (440/870) at León from 20 to 23 of February 2016.

The particular feature of the desert dust episode during February 2016 has also been shown by Sorribas et al. (2017), who studied the same event from historical datasets of meteorological variables, aerosol properties and ozone concentration at El Arenosillo observatory (southwestern Spain). In this work, a historical dataset (2006-2015) of February meteorological scenarios over North Africa evidenced the existence of airflows from the Sahel to Algeria and consequently temperature increases from the surface to 700 hPa by up to 7-9 ºC relative to the last decade. This phenomenon transports particles to the Iberian Peninsula at ground level and higher altitudes as Titos et al.,(2017) and Cazorla et al. (2017) showed in their studies carried out in different cities of Spain, between 20 and 24 February 2016. Similar episodes over the peninsula with AOD higher than 1 have been detected before, as the one in the summer of 2004, reaching an AOD of 2.7 (Cachorro et al., 2008). In this case, the desert dust was also mixed with smoke particles from concurrent forest fires in the Iberian Peninsula. Other extreme Saharan event were detected during September 2007 with AOD reaching 1.5 (Guerrero-Rascado et al., 2009). Nevertheless, the episodes were observed during warm seasons, not in the middle of winter, which illustrates the particularity of the present study.

4.3.2. Radiative forcing

One of the main effects of Saharan intrusions is the change in radiative forcing (Perrone and Bergamo, 2011). To underline the radiative forcing of these dust episodes we have computed mean aerosol daily radiative forcing over three specific periods (before, during and after the dust episode). These three periods are listed into the first column of the Table 5. Concerning the Saharan dust event in 2016 mean ΔF_{TOA} values vary from -21.8 before intrusion to -77.9 W m^{-2} during intrusion and mean ΔF_{BOA} values from -123.6 to -149.0 W m^{-2} (Table 5). These results indicate that the Saharan dust intrusion caused a cooling effect in the atmosphere (Perrone and Bergamo, 2011), with a mean heating

rate of -15.6 K day^{-1} during the dust event. Therefore, the Saharan intrusion influenced the radiative forcing in León, mainly decreasing the solar energy at surface. However, the energy in the atmosphere did not accumulate since the outgoing forcing at the top of the atmosphere was also intensified, losing much of the energy (lower values of ΔF_{ATM}). Besides, the optical properties during the event suggest also the change in absorbing capacities of the air mass, with an increase of *SSA* values (from 0.84 to 0.97 at 550 nm).

Concerning the Saharan dust event in 2017, the same pattern was observed, with the mean ΔF_{TOA} varying from -21.1 before intrusion to -84.1 W m^{-2} during intrusion and the mean ΔF_{BOA} from -52.1 to -164.9 W m^{-2} (Table 4). A cooling effect was also observed with a mean heating rate of -12.4 K day^{-1} during intrusion, lower than mean values for "before" and "after" periods. The optical properties during the event, such as *SSA* and *g* values did not present a large change that could support by itself the stronger scattering radiative effect, but the large variation of AOT between the "before", "during" and "after" period could explain the strong radiative signature of this event.

According to AEMET data, the visibility and the solar radiation in León were affected during both Saharan dust outbreaks. In days without dust intrusions, the visibility in León typically ranges between 50 and 60 km. However, during the event of 2016, the visibility decreased until 30 km. In the event of 2017, the decrease of the visibility was more evident, dropping to 24 km on 23 February at 0000-0700 UTC and to 10 km at 0700-1300 UTC, when the intrusion was at its peak. The negative impact of both events on visibility is comparable with that reported by Alonso-Blanco et al., (2018) during two large wildfires occurred at 70 km away from León city, causing a reduction in visibility from 78 km to 20 km. Regarding to solar radiation, during the day before the events, the direct total radiation was approximately 340 W m^{-2} in León, and the total daily diffuse radiation was about 20 W m^{-2}. During both Saharan dust intrusions, the direct total radiation decreases up to 71 W m^{-2} in 2016 and 140 W m^{-2} in 2017. Moreover, the total daily diffuse radiation increases up to 94 W m^{-2} and 87 W m^{-2} in 2016 and 2017, respectively. These results show that the contribution of solar diffuse radiation on global irradiance (direct + diffuse) increased (from 5% to 57% in 2016 and 38% in 2017) when the dust plume reached to León city. Similar results were obtained by Antón et al., (2012), which reported that the solar diffuse radiation contributed for almost 60% of the global radiation during an extreme Saharan dust event detected in September 2007 in Granada (Spain).

4.4. Bioaerosol characterization

The dust intrusions were also reflected in the pollen monitoring carried out at the sampling point, which highlights the modification of the population of both biological and non-biological particles due to long-range transport. During the Saharan dust intrusion studied in 2016 (between 21 and 22 February), sand particles and pollen grains not typical of flowering plants in this period of the year in the province of León were identified: i.e. *Artemisia* (17-28 µm) (Fig. 12b) and *Daphne* (18-23 µm). These pollen types are typical of the south of the Iberian Peninsula and the Mediterranean area, where they flourish in winter. Before and after the intrusion, a low concentration of pollen was detected with a predominance of Cupressaceae, *Corylus*, *Alnus* (13-18 µm) (Fig. 12a), and Poaceae (graminaceus). Other authors have reported the influence of the long-range transport in the presence of atypical pollen types and in the pollen concentration. Izquierdo et al. (2011) showed, for different long-range transport scenarios in summer of 1999 over Canary Island, Spain, the presence of several pollen types, such as *Artemisa*, *Olea*, *Quercus*, Poaceae,

Cyperaceae, among others. In Córdoba, Spain, Cariñanos et al. (2004) identified pollen types which did not correspond to the local pollen species or whose flowering period occurs at different periods of the year, in samples of the dust intrusion of summer 1999. *Cannabis*, *Sambucus*, *Pinus*, *Cupressus*, *Quercus* and *Fraxinus* were among the pollen types identified by these researchers.

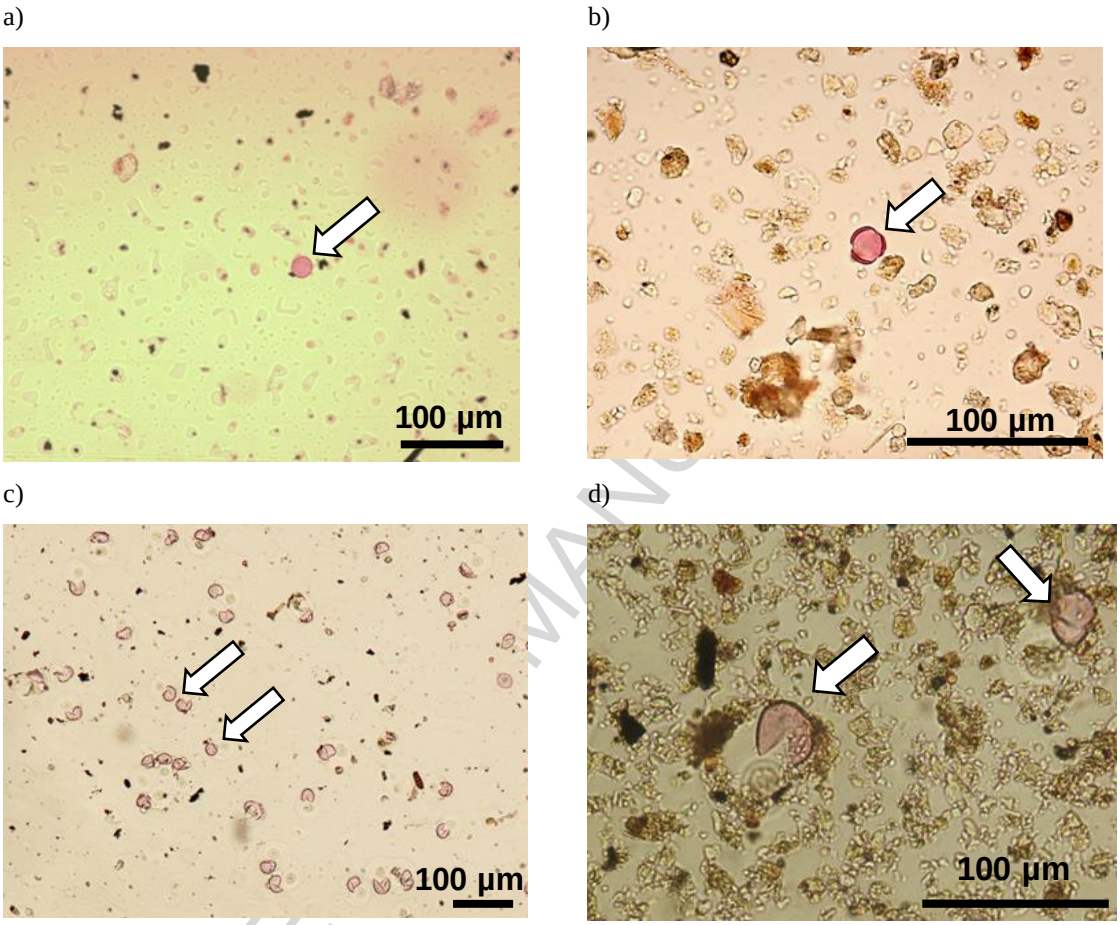

Fig. 12. Optical microscope images of pollen samples collected by the Hirst-type volumetric trap corresponding to a) 20/02/2016; b) 22/02/2016; c) 21/02/2017 and d) 23/02/2017 (a) and c) without dust intrusion and b) and d) under Sahara dust intrusion). The withe arrows indicate: a) *Corylus* b) *Artemisia* c) *Cupressaceae* [1] and *Poaceae* [2] pollen and d) *Cupressaceae* pollen.

Unlike the 2016 event, in 2017 the presence of atypical pollen types in León was not observed (Fig. 12 c and d). However, on 23 February 2017, when the dust plume reached the north of the Iberian Peninsula, the *Corylus* concentration was about six times higher (60 pollen m^{-3}) than the maximum value reached in previous days (10 pollen m^{-3}). From 24 February, the *Corylus* concentration in the atmosphere began to decline until it completely disappeared.

This behavior can be due to the trajectory of the air masses described in figure 3c, at 500 m level, that dragged large amounts of pollen emitted by the forests of the Cantabrian Mountains, located about 30 km north far from the city. Furthermore, the *Cupressaceae* pollen concentration decreased considerably during the dust intrusion (from 269 to 72 pollen m^{-3}). The presence of this type of pollen is very important in the east and central peninsula during this season since its flowering occurs earlier than in the city of León. The highest concentration of this type of pollen in the previous days is probably due to the trajectories of the air masses described above.

4.5. Inhalable, thoracic, tracheobronchial and respirable fractions

Changes in the aerosol size distribution caused for the dust plumes result in different amounts of mass deposited in the distinct zones of the respiratory tract. The results showed highest values of inhaled mass of aerosols during the days in which the dust plume was more intense in both February 2016 and 2017 (58 ± 11 and 52 ± 29 μg m^{-3}, respectively). These values are comparable with those obtained during summer 2012 in León city (43 μg m^{-3}) (Oduber et al., 2018), when the Saharan dust intrusions are more frequents (Table 5). Furthermore, the mass fraction of particles that could reach the alveolar area was higher during the intrusion days, due to the presence of a greater number of particles in the atmosphere. Values of respirable fraction, when the maximum particle mass concentration was reached in 2016, were 102 and 134 μg m^{-3} in healthy adults and in high-risk populations, respectively. In 2017, this value reached 155 μg m^{-3} in both healthy adults and in high-risk populations, respectively.

Table 3. Inhalable, thoracic, tracheobronchial and respirable mass fractions (μg m^{-3}) in healthy adults and high-risk population (children, frail or sick people), and maximum mass fraction values for the two study periods.

	Inhalable	**Thoracic**	**Tracheobronchial (μg m^{-3})**		**Respirable (μg m^{-3})**	
Date (Day)	**(μg m^{-3})**	**(μg m^{-3})**	**Healthy Adult**	**High Risk**	**Healthy Adult**	**High Risk**
February 2016						
20	18 ± 9	17 ± 8	3 ± 4	5 ± 4	14 ± 5	12 ± 4
21	**32 ± 29**	**31 ± 28**	**4 ± 4**	**9 ± 9**	**27 ± 24**	**22 ± 19**
22	**58 ± 11**	**55 ± 8**	**6 ± 1**	**15 ± 2**	**49 ± 7**	**40 ± 6**
23	17.5± 0.3	17.3 ± 0.5	1.5 ± 0.4	3.3 ± 0.4	15.8 ± 0.8	14.0 ± 0.8
Maximum (22, 1200 UTC)	156	153	19	51	134	102
February 2017						
21	10.0 ± 0.5	9.8 ± 0.2	0.6 ± 0.7	0.8 ± 0.9	9.2 ± 0.5	9.0 ± 0.6
22	**17 ± 12**	**16 ± 12**	**2 ± 1**	**3 ± 2**	**14 ± 10**	**13 ± 10**
23	**52 ± 29**	**52 ± 29**	**1 ± 2**	**2 ± 3**	**51 ± 31**	**50 ± 32**
24	14 ± 1	14 ± 1	4 ± 2	6 ± 3	10 ± 2	8 ± 4
Maximum (23, 1200 UTC)	155	155	0	0.01	155	155

5. Conclusions

Two unusual Saharan dust outbreaks arriving at León in February 2016 and 2017 were analyzed from a multidisciplinary perspective. In León city, the arrival of desert dust plumes resulted in the increase of the coarse fraction (D_p > 1µm) and in the exceedance of the PM_{10} DLV, with daily concentrations of 52 µg m^{-3} in 2016 and 86 µg m^{-3} in 2017, values even higher than those observed during summer Saharan dust intrusions of 2016 in the same city. Furthermore, a change in the biological material caused by long-range transport has been observed, evidenced by the presence of pollen grains not typical of flowering plants in this period in the province of León.

The rise in the iron concentration estimated from the aethalometer data, is consistent with the high contribution of dust in both outbreaks, reaching values up to 5.73 and 7.38 µg m^{-3} in 2016 and 2017, respectively. These results were also supported by the chemical analysis of the teflon filters sampled during the African intrusion of 2017, with daily Fe concentrations of 1.9 µg m^{-3} from the PIXE technique and 2.0 µg m^{-3} from the aethalometer data. Furthermore, the dust contribution in the event of 2017, was evidenced through the increase of the concentrations of the main elements associated with mineral sources (calcium, aluminum, titanium and silica), reaching values highest than those observed in summer Saharan dust intrusions in León during 2016. The total mineral fraction reached 44% of PM_{10} mass during the dust outbreak, while in the days before the dust intrusion, the mineral fraction reached mean values of 7%. It was also noted an increase in the SO_4^{2-}, NO_3^- and Cl^- concentrations during the Saharan dust intrusion.

During both dust events, the estimated mean aerosol radiative forcing values at the top and at the bottom of the atmosphere were of the same order. The presence of the dusty air masses resulted in decreasing the incoming solar flux at the surface. The energy did not accumulate in the atmosphere as mean atmospheric radiative forcing estimations decreased between the "during" and "before" and "after" periods. Consequently, the outgoing radiative fluxes at the top of the atmosphere were enhanced. The scattering optical properties at the origin of this cooling effect of the dust event were supported by the variation of the SSA values for the 2016 event, and by the large variation of the total amount of aerosol in the column, revealed through the AOT parameter evolution, for the 2017 event. The enhancement of the scattering property was also supported by the radiative surface measurements. Furthermore, on the 2016 event, AOD and extinction-related Ångström exponent showed clearly characteristics of desert aerosol, registering values of 1.1 and 0.05, respectively.

The impact on the respiratory tract regions of the high levels of particulate matter during both Saharan dust intrusions was estimated using the International Organization for Standardization. The highest values of inhaled mass of aerosols were 58 ± 11 and 52 ± 29 µg m^{-3}, during the 2016 and 2017 outbreaks, respectively, with values of respirable fraction of 102 and 134 µg m^{-3} in healthy adults and high-risk populations, respectively in 2016. In 2017, these values reached approximately 155 µg m^{-3} in healthy adults and high-risk populations. These concentrations are approximately 9 times the mean value recorded in days without dust intrusion, showing that these natural events can cause a negative impact on human health.

This kind of complete descriptive studies is essential not only for air quality and transport understandings but also for the subsequent implications on health and climate, two main targets of policy makers. An integrative approach should be performed through modeling exercises to go on understanding the dynamic, radiative, and transport feedback loops and their impact on air quality and health.

Acknowledgments

This study was partially supported by the Spanish Ministry of Economy and Competitiveness (Grant TEC2014-57821-R), the University of León (Programa Propio 2015/00054/001 and 2018/00203/001) and the AERORAIN project (Ministry of Economy and Competitiveness, Grant CGL2014-52556-R, co-financed with European FEDER funds). F. Oduber acknowledges the grant BES-2015-074473 from the Spanish Ministry of Economy and Competitiveness. C. Blanco-Alegre acknowledges the grant FPU16-05764 from the Spanish Ministry of Education, Culture and Sport. The authors gratefully acknowledge the NOAA Air Resources Laboratory (ARL) for the provision of the HYSPLIT transport and dispersion model and/or READY website (http://www.ready.noaa.gov) used in this study. The authors would also like to express their gratitude to the Naval Research Laboratory for providing the NAAP aerosol map and NASA for the satellite image used in the graphical abstract. The data from the MAPAMA network are property of the Office for Quality and Environmental Evaluation (DGCEA, in its Spanish acronym), belonging to the Ministry of Ecologic Transition. The data were supplied as a result of an agreement between the Spanish Ministry of Agriculture, Food and the Environment and the Scientific Research Council for sponsoring studies related to air pollution by particulate matter and metals in Spain. We thank AERONET network and specially Victoria E. Cachorro Revilla and Carlos Toledano for establishing and maintaining the Valladolid AERONET site used in this investigation. We also thank to Philippe Dubuisson for allowing the use of GAME model, as well as the Laboratoire d'Optique Atmosphérique (University of Lille).

References

Alastuey, A., Querol, X., Aas, W., Lucarelli, F., Pérez, N., Moreno, T., Cavalli, F., Areskoug, H., Balan, V., Catrambone, M., Ceburnis, D., Cerro, J.C., Conil, S., Gevorgyan, L., Hueglin, C., Imre, K., Jaffrezo, J.-L., Leeson, S.R., Mihalopoulos, N., Mitosinkova, M., O'Dowd, C.D., Pey, J., Putaud, J.-P., Riffault, V., Ripoll, A., Sciare, J., Sellegri, K., Spindler, G., Yttri, K.E., 2016. Geochemistry of PM10 over Europe during the EMEP intensive measurement periods in summer 2012 and winter 2013. Atmos. Chem. Phys. 16, 6107–6129. doi:10.5194/acp-16-6107-2016

Alonso-Blanco, E., Castro, A., Calvo, A.I., Pont, V., Mallet, M., Fraile, R., 2018. Wildfire smoke plumes transport under a subsidence inversion: Climate and health implications in a distant urban area. Sci. Total Environ. 619–620, 988–1002. doi:10.1016/j.scitotenv.2017.11.142

Alonso-Blanco, E., Gómez-Moreno, F.J., Núñez, L., Pujadas, M., Cusack, M., Artíñano, B., 2017. Corrigendum to "Aerosol particle shrinkage event phenomenology in a South European suburban area during 2009–2015" [Atmos. Environ. 160C (2017) 154–164]. Atmos. Environ. 164, 476. doi:10.1016/j.atmosenv.2017.05.045

Alves, C., Calvo, A.I., Marques, L., Castro, A., Nunes, T., Coz, E., Fraile, R., 2014. Particulate matter in the indoor and outdoor air of a gymnasium and a fronton. Environ. Sci. Pollut. Res. 21, 12390–12402. doi:10.1007/s11356-014-3168-1

Alves, C.A., Lopes, D.J., Calvo, A.I., Evtyugina, M., Rocha, S., Nunes, T., 2015. Emissions from Light-Duty Diesel and Gasoline in-use Vehicles Measured on Chassis Dynamometer Test Cycles. Aerosol Air Qual. Res. 15, 99–116. doi:10.4209/aaqr.2014.01.0006

Ansmann, A., Bösenberg, J., Chaikovsky, A., Comerón, A., Eckhardt, S., Eixmann, R., Freudenthaler, V., Ginoux, P., Komguem, L., Linné, H., Márquez, M.Á.L., Matthias, V., Mattis, I., Mitev, V., Müller, D., Music, S., Nickovic, S., Pelon, J., Sauvage, L., Sobolewsky, P., Srivastava, M.K., Stohl, A., Torres, O., Vaughan, G., Wandinger, U., Wiegner, M., 2003. Long-range transport of Saharan dust to northern Europe: The 11-16 October 2001 outbreak observed with EARLINET. J. Geophys. Res. Atmos. 108. doi:10.1029/2003JD003757

Antón, M., Valenzuela, A., Cazorla, A., Gil, J.E., Fernández-Gálvez, J., Lyamani, H., Foyo-Moreno, I., Olmo, F.J., Alados-Arboledas, L., 2012. Global and diffuse shortwave irradiance during a strong desert dust episode at Granada (Spain). Atmos. Res. 118, 232–239. doi:10.1016/j.atmosres.2012.07.007

Artíñano, B., Salvador, P., Alonso, D.G., Querol, X., Alastuey, A., 2003. Anthropogenic and natural influence on the PM10 and PM2.5 aerosol in Madrid (Spain). Analysis of high concentration episodes. Environ. Pollut. 125, 453–465. doi:10.1016/S0269-7491(03)00078-2

Aymoz, G., Jaffrezo, J., Jacob, V., Colomb, A., George, C., 2004. Evolution of organic and inorganic components of aerosol during a Saharan dust episode observed in the French Alps. Atmos. Chem. Phys. 2499–2512.

Blanco-Alegre, C., Calvo, A.I., Coz, E., Castro, A., Oduber, F., Prévôt, A.S.H., Močnik, G., Fraile, R., 2019. Quantification of source specific black carbon scavenging using an aethalometer and a disdrometer. Environ. Pollut. 246, 336–345. doi:10.1016/j.envpol.2018.11.102

Bond, T.C., 2001. Spectral dependence of visible light absorption by carbonaceous particles emitted from coal combustion. Geophys. Res. Lett. 28, 4075–4078. doi:10.1029/2001GL013652

Cachorro, V.E., Toledano, C., Prats, N., Sorribas, M., Mogo, S., Berjón, A., Torres, B., Rodrigo, R., de la Rosa, J., De Frutos, A.M., 2008. The strongest desert dust intrusion mixed with smoke over the Iberian Peninsula registered with Sun photometry. J. Geophys. Res. 113, D14S04. doi:10.1029/2007JD009582

Calvo, A.I., Alves, C., Castro, A., Pont, V., Vicente, A.M., Fraile, R., 2013. Research on aerosol sources and chemical composition: Past, current and emerging issues. Atmos. Res. 120–121, 1–28. doi:10.1016/j.atmosres.2012.09.021

Calvo, A.I., Pont, V., Castro, A., Mallet, M., Palencia, C., Roger, J.C., Dubuisson, P., Fraile, R., 2010. Radiative

forcing of haze during a forest fire in Spain. J. Geophys. Res. 115, D08206. doi:10.1029/2009JD012172

Caquineau, S., Gaudichet, A., Gomes, L., Magonthier, M.-C., Chatenet, B., 1998. Saharan dust: Clay ratio as a relevant tracer to assess the origin of soil-derived aerosols. Geophys. Res. Lett. 25, 983–986. doi:10.1029/98GL00569

Cariñanos, P., Galán, C., Alcázar, P., Domínguez, E., 2004. Analysis of the particles transported with dust-clouds reaching Cordoba, Southwestern Spain. Arch. Environ. Contam. Toxicol. 46, 141–146. doi:10.1007/s00244-003-2273-9

Castro, A., Alonso-Blanco, E., González-Colino, M., Calvo, A.I., Fernández-Raga, M., Fraile, R., 2010. Aerosol size distribution in precipitation events in León, Spain. Atmos. Res. 96, 421–435. doi:10.1016/j.atmosres.2010.01.014

Castro, A., Calvo, A.I., Alves, C., Alonso-Blanco, E., Coz, E., Marques, L., Nunes, T., Fernández-Guisuraga, J.M., Fraile, R., 2015. Indoor aerosol size distributions in a gymnasium. Sci. Total Environ. 524–525, 178–186. doi:10.1016/j.scitotenv.2015.03.118

Castro, A., Calvo, A.I., Blanco-Alegre, C., Oduber, F., Alves, C., Coz, E., Amato, F., Querol, X., Fraile, R., 2018. Impact of the wood combustion in an open fireplace on the air quality of a living room: Estimation of the respirable fraction. Sci. Total Environ. 628–629, 169–176. doi:10.1016/j.scitotenv.2018.02.001

Cazorla, A., Casquero-Vera, J.A., Román, R., Guerrero-Rascado, J.L., Toledano, C., Cachorro, V.E., Orza, J.A.G., Cancillo, M.L., Serrano, A., Titos, G., Pandolfi, M., Alastuey, A., Hanrieder, N., Alados-Arboledas, L., 2017. Near-real-time processing of a ceilometer network assisted with sun-photometer data: mnitoring a dust outbreak over the Iberian Peninsula. Atmos. Chem. Phys. 17, 11861–11876. doi:10.5194/acp-2017-151

Charron, A., Harrison, R.M., 2003. Primary particle formation from vehicle emissions during exhaust dilution in the roadside atmosphere. Atmos. Environ. 37, 4109–4119. doi:10.1016/S1352-2310(03)00510-7

Córdoba-Jabonero, C., Sorribas, M., Guerrero-Rascado, J.L., Adame, J.A., Hernández, Y., Lyamani, H., Cachorro, V., Gil, M., Alados-Arboledas, L., Cuevas, E., de la Morena, B., 2011. Synergetic monitoring of Saharan dust plumes and potential impact on surface: a case study of dust transport from Canary Islands to Iberian Peninsula. Atmos. Chem. Phys. 11, 3067–3091. doi:10.5194/acp-11-3067-2011

Coz, E., Gómez-Moreno, F.J., Casuccio, G.S., Artíñano, B., 2010. Variations on morphology and elemental composition of mineral dust particles from local, regional, and long-range transport meteorological scenarios. J. Geophys. Res. Atmos. 115, 1–12. doi:10.1029/2009JD012796

Coz, E., Gómez-Moreno, F.J., Pujadas, M., Casuccio, G.S., Lersch, T.L., Artíñano, B., 2009. Individual particle characteristics of North African dust under different long-range transport scenarios. Atmos. Environ. 43, 1850–

1863. doi:10.1016/j.atmosenv.2008.12.045

Denjean, C., Cassola, F., Mazzino, A., Triquet, S., Chevaillier, S., Grand, N., Bourrianne, T., Momboisse, G., Sellegri, K., Schwarzenbock, A., Freney, E., Mallet, M., Formenti, P., 2016. Size distribution and optical properties of mineral dust aerosols transported in the western Mediterranean. Atmos. Chem. Phys. 16, 1081–1104. doi:10.5194/acp-16-1081-2016

Dentener, F.J., Carmichael, G.R., Zhang, Y., Lelieveld, J., Crutzen, P.J., 1996. Role of mineral aerosol as a reactive surface in the global troposphere. J. Geophys. Res. Atmos. 101, 22869–22889. doi:10.1029/96JD01818

Díaz, J., Linares, C., Carmona, R., Russo, A., Ortiz, C., Salvador, P., Trigo, R.M., 2017. Saharan dust intrusions in Spain: Health impacts and associated synoptic conditions. Environ. Res. 156, 455–467. doi:10.1016/j.envres.2017.03.047

Draxler, R., Rolph, G., 2012. Hysplit (Hybrid Single-Particle Lagrangian Integrated Trajectory). Silver Spring. NOAA Air Resour. Lab.

Dubuisson, P., Buriez, J.C., Fouquart, Y., 1996. High spectral resolution solar radiative transfer in absorbing and scattering media: Application to the satellite simulation. J. Quant. Spectrosc. Radiat. Transf. 55, 103–126. doi:10.1016/0022-4073(95)00134-4

Dubuisson, P., Dessailly, D., Vesperini, M., Frouin, R., 2004. Water vapor retrieval over ocean using near-infrared radiometry. J. Geophys. Res. D Atmos. 109, 1–14. doi:10.1029/2004JD004516

Dunn, O.J., 1964. Multiple Comparisons Using Rank Sums. Technometrics 6, 241–252. doi:10.1080/00401706.1964.10490181

Escudero, M., Querol, X., Ávila, A., Cuevas, E., 2007. Origin of the exceedances of the European daily PM limit value in regional background areas of Spain. Atmos. Environ. 41, 730–744. doi:10.1016/j.atmosenv.2006.09.014

Estellés, V., Campanelli, M., Smyth, T.J., Utrillas, M.P., Martínez-Lozano, J.A., 2012. Evaluation of the new ESR network software for the retrieval of direct sun products from CIMEL CE318 and PREDE POM01 sun-sky radiometers. Atmos. Chem. Phys. 12, 11619–11630. doi:10.5194/acp-12-11619-2012

Fialho, P., Cerqueira, M., Pio, C., Cardoso, J., Nunes, T., Custódio, D., Alves, C., Almeida, S.M., Almeida-Silva, M., Reis, M., Rocha, F., 2014. The application of a multi-wavelength aethalometer to estimate iron dust and black carbon concentrations in the marine boundary layer of cape verde. Atmos. Environ. 97, 136–143. doi:10.1016/j.atmosenv.2014.08.008

Fialho, P., Freitas, M.C., Barata, F., Vieira, B., Hansen, A.D.A., Honrath, R.E., 2006. The Aethalometer calibration

and determination of iron concentration in dust aerosols. J. Aerosol Sci. 37, 1497–1506. doi:10.1016/j.jaerosci.2006.03.002

Fubini, B., Otero Areán, C., 1999. Chemical aspects of the toxicity of inhaled mineral dusts. Chem. Soc. Rev. 28, 373–381. doi:10.1039/a805639k

Galán Soldevilla, C., Cariñanos González, P., Alcázar Teno, P., Domínguez Vilches, E., 2007. Spanish Aerobiology Network (REA): management and quality manual.

Galindo, N., Nicolás, J.F., Yubero, E., Caballero, S., Pastor, C., Crespo, J., 2008. Factors affecting levels of aerosol sulfate and nitrate on the Western Mediterranean coast. Atmos. Res. 88, 305–313. doi:10.1016/j.atmosres.2007.11.024

Garrison, V.H., Foreman, W.T., Genualdi, S., Griffin, D.W., Kellogg, C.A., Majewski, M.S., Mohammed, A., Ramsubhag, A., Shinn, E.A., Simonich, S.L., Smith, G.W., 2006. Saharan dust – a carrier of persistent organic pollutants, metals and microbes to the Caribbean? Int. J. Trop. Biol. Conserv. 54, 9–21.

Glaccum, R.A., Prospero, J.M., 1980. Saharan aerosols over the tropical North Atlantic — Mineralogy. Mar. Geol. 37, 295–321. doi:10.1016/0025-3227(80)90107-3

Goudie, A.S., 2014. Desert dust and human health disorders. Environ. Int. 63, 101–113. doi:10.1016/j.envint.2013.10.011

Griffin, D.W., 2007. Atmospheric Movement of Microorganisms in Clouds of Desert Dust and Implications for Human Health. Clin. Microbiol. Rev. 20, 459–477. doi:10.1128/CMR.00039-06

Griffin, D.W., Kellogg, C.A., Shinn, E.A., 2001. Dust in the wind: Long range transport of dust in the atmosphere and its implications for global public and ecosystem health. Glob. Chang. Hum. Heal. 2, 20–33.

Guerrero-Rascado, J.L., Olmo, F.J., Avilés-Rodríguez, I., Navas-Guzmán, F., Pérez-Ramírez, D., Lyamani, H., Alados Arboledas, L., 2009. Extreme Saharan dust event over the southern Iberian Peninsula in september 2007: active and passive remote sensing from surface and satellite. Atmos. Chem. Phys. 9, 8453–8469. doi:10.5194/acp-9-8453-2009

Guerzoni, S., Molinaroli, E., Chester, R., 1997. Saharan dust inputs to the western Mediterranean Sea: depositional patterns, geochemistry and sedimentological implications. Deep. Res. II 44, 631–654.

Guieu, C., Bozec, Y., Blain, S., Ridame, C., Sarthou, G., Leblond, N., 2002. Impact of high Saharan dust inputs on dissolved iron concentrations in the Mediterranean Sea. Geophys. Res. Lett. 29, 17-1-17–4. doi:10.1029/2001GL014454

Holben, B.N., Eck, T.F., Slutsker, I., Tanré, D., Buis, J.P., Setzer, A., Vermote, E., Reagan, J.A., Kaufman, Y.J.,

Nakajima, T., Lavenu, F., Jankowiak, I., Smirnov, A., 1998. AERONET-A Federated Instrument Network and Data Archive for Aerosol Characterization. Remote Sens. Environ. 66, 1–16.

International Organization for Standardization, 1995. ISO 7708: 1995 Air quality -Particle size fraction definitions for health-related sampling. ISO Publications, 1st edition, 1995-04-01.

IPCC, 2014. Climate change 2014: Impacts, adaptation, and vulnerability. Part A: Global and sectoral aspects. Contribution of working group II to the fifth assessment report of the intergovernmental panel on climate change.

Izquierdo, R., Belmonte, J., Avila, A., Alarcón, M., Cuevas, E., Alonso-Pérez, S., 2011. Source areas and long-range transport of pollen from continental land to Tenerife (Canary Islands). Int. J. Biometeorol. 55, 67–85. doi:10.1007/s00484-010-0309-1

Jiménez, E., Linares, C., Martínez, D., Díaz, J., 2010. Role of Saharan dust in the relationship between particulate matter and short-term daily mortality among the elderly in Madrid (Spain). Sci. Total Environ. 408, 5729–5736. doi:10.1016/j.scitotenv.2010.08.049

Kruskal, W.H., Wallis, W.A., 1952. Use of Ranks in One-Criterion Variance Analysis. J. Am. Stat. Assoc. 47, 583–621. doi:10.1080/01621459.1952.10483441

Levin, E.J.T., McMeeking, G.R., Carrico, C.M., Mack, L.E., Kreidenweis, S.M., Wold, C.E., Moosmüller, H., Arnott, W.P., Hao, W.M., Collett, J.L., Malm, W.C., 2010. Biomass burning smoke aerosol properties measured during Fire Laboratory at Missoula Experiments (FLAME). J. Geophys. Res. 115, D18210. doi:10.1029/2009JD013601

Liao, H., Adams, P.J., Chung, S.H., Seinfeld, J.H., Mickley, L., Jacob, D., 2003. Interactions between tropospheric chemistry and aerosols in a unified general circulation model. J. Geophys. Res. 108, 4001. doi:10.1029/2001JD001260

López-Villarrubia, E., Iñiguez, C., Peral, N., García, M.D., Ballester, F., 2012. Characterizing mortality effects of particulate matter size fractions in the two capital cities of the Canary Islands. Environ. Res. 112, 129–138. doi:10.1016/j.envres.2011.10.005

Lucarelli, F., Chiari, M., Calzolai, G., Giannoni, M., Nava, S., Udisti, R., Severi, M., Querol, X., Amato, F., Alves, C., Eleftheriadis, K., 2015. The role of PIXE in the AIRUSE project "testing and development of air quality mitigation measures in Southern Europe." Nucl. Instruments Methods Phys. Res. Sect. B Beam Interact. with Mater. Atoms 363, 92–98. doi:10.1016/j.nimb.2015.08.023

Lyamani, H., Valenzuela, A., Perez-Ramirez, D., Toledano, C., Granados-Muñoz, M.J., Olmo, F.J., Alados-Arboledas, L., 2015. Aerosol properties over the western Mediterranean basin: temporal and spatial variability.

Atmos. Chem. Phys. 15, 2473–2486. doi:10.5194/acp-15-2473-2015

Morawska, L., Salthammer, T., 2003. Indoor Environment, Indoor Environment: Airborne Particles and Settled Dust. Wiley-VCH Verlag GmbH & Co. KGaA, Weinheim, Germany. doi:10.1002/9783527610013

Nicolás, J., Chiari, M., Crespo, J., Orellana, I.G., Lucarelli, F., Nava, S., Pastor, C., Yubero, E., 2008. Quantification of Saharan and local dust impact in an arid Mediterranean area by the positive matrix factorization (PMF) technique. Atmos. Environ. 42, 8872–8882. doi:10.1016/j.atmosenv.2008.09.018

NOAA, n.d. Passive Cavity Aerosol Spectrometer Probe (PCASP) [WWW Document]. URL https://www.esrl.noaa.gov/gmd/aero/instrumentation/pcasp100.html (accessed 12.12.18).

Oduber, F., Calvo, A.I., Blanco-Alegre, C., Castro, A., Vega-Maray, A.M., Valencia-Barrera, R.M., Fernández-González, D., Fraile, R., 2019. Links between recent trends in airborne pollen concentration, meteorological parameters and air pollutants. Agric. For. Meteorol. 264, 16–26. doi:10.1016/j.agrformet.2018.09.023

Oduber, F., Castro, A., Calvo, A.I., Blanco-Alegre, C., Alonso-Blanco, E., Belmonte, P., Fraile, R., 2018. Summer-autumn air pollution in León, Spain: changes in aerosol size distribution and expected effects on the respiratory tract. Air Qual. Atmos. Heal. 11, 505–520. doi:10.1007/s11869-018-0556-6

Olson, M.R., Victoria Garcia, M., Robinson, M.A., Van Rooy, P., Dietenberger, M.A., Bergin, M., Schauer, J.J., 2015. Investigation of black and brown carbon multiple-wavelength-dependent light absorption from biomass and fossil fuel combustion source emissions. J. Geophys. Res. Atmos. 120, 6682–6697. doi:10.1002/2014JD022970

Oteros, J., Buters, J., Laven, G., Röseler, S., Wachter, R., Schmidt-Weber, C., Hofmann, F., 2017. Errors in determining the flow rate of Hirst-type pollen traps. Aerobiologia (Bologna). 33, 201–210. doi:10.1007/s10453-016-9467-x

Perez, L., Tobias, A., Querol, X., Künzli, N., Pey, J., Alastuey, A., Viana, M., Valero, N., González-Cabré, M., Sunyer, J., 2008. Coarse Particles From Saharan Dust and Daily Mortality. Epidemiology 19, 800–807. doi:10.1097/EDE.0b013e31818131cf

Perrone, M.R., Bergamo, A., 2011. Direct radiative forcing during Sahara dust intrusions at a site in the Central Mediterranean: Anthropogenic particle contribution. Atmos. Res. 101, 783–798. doi:10.1016/j.atmosres.2011.05.011

Pio, C., Cerqueira, M., Harrison, R.M., Nunes, T., Mirante, F., Alves, C., Oliveira, C., Sanchez de la Campa, A., Artíñano, B., Matos, M., 2011. OC/EC ratio observations in Europe: Re-thinking the approach for apportionment between primary and secondary organic carbon. Atmos. Environ. 45, 6121–6132. doi:10.1016/j.atmosenv.2011.08.045

Polymenakou, P.N., Mandalakis, M., Stephanou, E.G., Tselepides, A., 2007. Particle Size Distribution of Airborne Microorganisms and Pathogens during an Intense African Dust Event in the Eastern Mediterranean. Environ. Health Perspect. 116, 292–296. doi:10.1289/ehp.10684

Putaud, J.-P., Van Dingenen, R., Mangoni, M., Virkkula, A., Raes, F., Maring, H., Prospero, J.M., Swietlicki, E., Berg, O.H., Hillamo, R., Mäkelä, T., 2000. Chemical mass closure and assessment of the origin of the submicron aerosol in the marine boundary layer and the free troposphere at Tenerife during ACE-2. Tellus B Chem. Phys. Meteorol. 52, 141–168. doi:10.3402/tellusb.v52i2.16090

Querol, X., Alastuey, A., Pandolfi, M., Reche, C., Pérez, N., Minguillón, M.C., Moreno, T., Viana, M., Escudero, M., Orio, A., Pallarés, M., Reina, F., 2014. 2001–2012 trends on air quality in Spain. Sci. Total Environ. 490, 957–969. doi:10.1016/j.scitotenv.2014.05.074

Querol, X., Alastuey, A., Rodríguez, S., Viana, M.M., Artíñano, B., Salvador, P., Mantilla, E., do Santos, S.G., Patier, R.F., de La Rosa, J., de la Campa, A.S., Menéndez, M., Gil, J.J., 2004a. Levels of particulate matter in rural, urban and industrial sites in Spain. Sci. Total Environ. 334–335, 359–376. doi:10.1016/j.scitotenv.2004.04.036

Querol, X., Alastuey, A., Ruiz, C.R., Artiñano, B., Hansson, H.C., Harrison, R.M., Buringh, E., ten Brink, H.M., Lutz, M., Bruckmann, P., Straehl, P., Schneider, J., 2004b. Speciation and origin of PM10 and PM2.5 in selected European cities. Atmos. Environ. 38, 6547–6555. doi:10.1016/j.atmosenv.2004.08.037

Rodríguez, S., Querol, X., Alastuey, A., Kallos, G., Kakaliagou, O., 2001. Saharan dust contributions to PM10 and TSP levels in Southern and Eastern Spain. Atmos. Environ. 35, 2433–2447. doi:10.1016/S1352-2310(00)00496-9

Rolph, G., Stein, A., Stunder, B., 2017. Real-time Environmental Applications and Display sYstem: READY. Environ. Model. Softw. 95, 210–228. doi:10.1016/j.envsoft.2017.06.025

Salvador, P., Artíñano, B., Molero, F., Viana, M., Pey, J., Alastuey, A., Querol, X., 2013. African dust contribution to ambient aerosol levels across central Spain: Characterization of long-range transport episodes of desert dust. Atmos. Res. 127, 117–129. doi:10.1016/j.atmosres.2011.12.011

Sandradewi, J., Prévôt, A.S.H., Szidat, S., Perron, N., Alfarra, M.R., Lanz, V.A., Weingartner, E., Baltensperger, U.R.S., 2008. Using aerosol light abosrption measurements for the quantitative determination of wood burning and traffic emission contribution to particulate matter. Environ. Sci. Technol. doi:10.1021/es702253m

Schütz, L., Sebert, M., 1987. Mineral aerosol and source identification. J. Aerosol Sci. 18, 1–10.

Sorribas, M., Adame, J.A., Andrews, E., Yela, M., 2017. An anomalous African dust event and its impact on aerosol radiative forcing on the Southwest Atlantic coast of Europe in February 2016. Sci. Total Environ. 583, 269–

279. doi:10.1016/j.scitotenv.2017.01.064

Stafoggia, M., Zauli-Sajani, S., Pey, J., Samoli, E., Alessandrini, E., Basagaña, X., Cernigliaro, A., Chiusolo, M., Demaria, M., Díaz, J., Faustini, A., Katsouyanni, K., Kelessis, A.G., Linares, C., Marchesi, S., Medina, S., Pandolfi, P., Pérez, N., Querol, X., Randi, G., Ranzi, A., Tobias, A., Forastiere, F., 2015. Desert Dust Outbreaks in Southern Europe: Contribution to Daily PM10 Concentrations and Short-Term Associations with Mortality and Hospital Admissions. Environ. Health Perspect. 124, 413–419. doi:10.1289/ehp.1409164

Stein, A.F., Draxler, R.R., Rolph, G.D., Stunder, B.J.B., Cohen, M.D., Ngan, F., 2015. NOAA's HYSPLIT Atmospheric Transport and Dispersion Modeling System. Bull. Am. Meteorol. Soc. 96, 2059–2077. doi:10.1175/BAMS-D-14-00110.1

Struckmeier, C., Drewnick, F., Fachinger, F., Gobbi, G.P., Borrmann, S., 2016. Atmospheric aerosols in Rome, Italy: sources, dynamics and spatial variations during two seasons. Atmos. Chem. Phys. 16, 15277–15299. doi:10.5194/acp-16-15277-2016

Takamura, T., Nakajima, T., 2004. Overview of SKYNET and its Activities. J. Pure Appl. Opt. 37, 3303–3308.

Titos, G., Ealo, M., Pandolfi, M., Pérez, N., Sola, Y., Sicard, M., Comerón, A., Querol, X., Alastuey, A., 2017. Spatiotemporal evolution of a severe winter dust event in the western Mediterranean: Aerosol optical and physical properties. J. Geophys. Res. Atmos. 122, 4052–4069. doi:10.1002/2016JD026252

Tobías, A., Pérez, L., Díaz, J., Linares, C., Pey, J., Alastruey, A., Querol, X., 2011. Short-term effects of particulate matter on total mortality during Saharan dust outbreaks: A case-crossover analysis in Madrid (Spain). Sci. Total Environ. 412–413, 386–389. doi:10.1016/j.scitotenv.2011.10.027

Tomadin, L., Cesari, G., Fuzzi, S., Lobietti, A., Mandrioli, P., Lenaz, R., Landuzzi, V., Mariotti, M., Mazzucotelli, A., Vannucci, R., 1989. Eolian Dust Collected in Springtime (1979 and 1984 Years) at the Seawater-Air Interface of the Northern Red Sea, in: Leinen, M., Sarnthein, M. (Eds.), Paleoclimatology and Paleometeorology: Modern and Past Patterns of Global Atmospheric Transport. Springer Netherlands, Dordrecht, pp. 283–310. doi:10.1007/978-94-009-0995-3_12

UNI 11108:2004, 2004. Air quality: Method for sampling and counting of airborne pollen grains and fungal spores.

Viana, M., Pey, J., Querol, X., Alastuey, A., de Leeuw, F., Lükewille, A., 2014. Natural sources of atmospheric aerosols influencing air quality across Europe. Sci. Total Environ. 472, 825–833. doi:10.1016/j.scitotenv.2013.11.140

Viana, M., Querol, X., Alastuey, A., Cuevas, E., Rodríguez, S., 2002. Influence of African dust on the levels of atmospheric particulates in the Canary Islands air quality network. Atmos. Environ. 36, 5861–5875. doi:10.1016/S1352-2310(02)00463-6

Wehner, B., Wiedensohler, A., 2002. Long term measurements of submicrometer urban aerosols: statistical analysis for correlations with meteorological conditions and trace gases. Atmos. Chem. Phys. Discuss. 2, 1699–1733. doi:10.5194/acpd-2-1699-2002

Weingartner, E., Saathoff, H., Schnaiter, M., Streit, N., Bitnar, B., Baltensperger, U., 2003. Absorption of light by soot particles: determination of the absorption coefficient by means of aethalometers. J. Aerosol Sci. 34, 1445–1463. doi:10.1016/S0021-8502(03)00359-8

Wiedensohler, A., Birmili, W., Nowak, A., Sonntag, A., Weinhold, K., Merkel, M., Wehner, B., Tuch, T., Pfeifer, S., Fiebig, M., Fjäraa, A.M., Asmi, E., Sellegri, K., Depuy, R., Venzac, H., Villani, P., Laj, P., Aalto, P., Ogren, J.A., Swietlicki, E., Williams, P., Roldin, P., Quincey, P., Hüglin, C., Fierz-Schmidhauser, R., Gysel, M., Weingartner, E., Riccobono, F., Santos, S., Grüning, C., Faloon, K., Beddows, D., Harrison, R., Monahan, C., Jennings, S.G., O'Dowd, C.D., Marinoni, A., Horn, H.-G., Keck, L., Jiang, J., Scheckman, J., McMurry, P.H., Deng, Z., Zhao, C.S., Moerman, M., Henzing, B., de Leeuw, G., Löschau, G., Bastian, S., 2012. Mobility particle size spectrometers: harmonization of technical standards and data structure to facilitate high quality long-term observations of atmospheric particle number size distributions. Atmos. Meas. Tech. 5, 657–685. doi:10.5194/amt-5-657-2012

Yang, M., Howell, S.G., Zhuang, J., Huebert, B.J., 2009. Attribution of aerosol light absorption to black carbon, brown carbon, and dust in China - Interpretations of atmospheric measurements during EAST-AIRE. Atmos. Chem. Phys. 9, 2035–2050. doi:10.5194/acp-9-2035-2009

Graphical abstract

Highlights

- Winter Saharan dust outbreaks brought pollen grains not typical of NW Spain.
- Increases of columnar AOD and exceedances of the daily PM_{10} limit value were recorded.
- PIXE analysis and aethalometer data confirmed a rise in the iron concentration.
- Dusty air masses caused a decreasing of the incoming solar flux at the surface.
- The respirable mass fraction was 9 times higher than those recorded the days before.